Åbo Akademi University

Faculty of Science and Engineering

Solid-contact ion-selective electrodes with high sensitivity – comparison of potentiometric and coulometric signal transduction

Master's thesis Project

30 ECTS

Nikola Obradović

Åbo

June, 2019

Co-funded by the
Erasmus+ Programme
of the European Union

Supervisor:

Dr. Zekra Mousavi, senior researcher

Laboratory of Analytical Chemistry (Åbo Akademi University)

Co-supervisors:

Dr. Tomasz Sokalski, senior researcher

Laboratory of Analytical Chemistry (Åbo Akademi University)

Prof. Ivo Leito

Institute of Chemistry (University of Tartu)

Examiner:

Prof. Johan Bobacka

Laboratory of Analytical Chemistry (Åbo Akademi University)

Date of the defense

4 June 2019

Abstract

In this research work, the novel coulometric signal transduction method, recently developed for improving the precision of ion sensing, was further investigated. Potassium-, hydrogen-, and chloride- solid-contact ion-selective electrodes (SCISEs) were prepared and studied in this work. The conducting polymer poly(3,4-ethylenedioxythiophene) (PEDOT), doped either with poly(styrene sulfonate) (PSS), *i.e.* PEDOT:PSS , or chloride (Cl^-), *i.e.* PEDOT:Cl^-, was used as ion-to-electron transducer in the prepared SCISEs. By using sequential addition-dilution procedure, the electrodes were tested using the two-electrode potentiometric, and three-electrode coulometric (chronoamperometric) signal transduction methods. The measurements were carried out in solutions with and without interfering ions. The results for potassium SCISEs show that small changes of potassium ion concentration cannot be monitored by potentiometry, while clear current (charge) peaks are observed when using the coulometric signal transduction method. Electrochemical impedance spectroscopy (EIS) was used to probe the theoretical concept of RC circuit that was recently developed for chloride SCISEs in coulometric signal transduction. With capacitance of the solid-contact and the thickness of the ion-selective membrane (ISM) kept constant, all three types of SCISEs imply the presence of correlation between the equilibration times and the resistances of the ISMs. To test this further, the electrodes with PEDOT:PSS and PEDOT:Cl^- solid-contacts, without ISMs, were exposed to changes in potassium, hydrogen and chloride concentrations. In this case, the PEDOT:PSS electrodes behaved according to the ionic mobilities of hydrogen and potassium ions, with the equilibration times for potassium ions being five times higher than those for hydrogen ions. On the contrary, equilibration times with PEDOT:Cl^- electrodes were comparably fast, almost instantaneous, for chloride ions, clearly showing a different ionic transduction in PEDOT:Cl^- compared to PEDOT:PSS. By performing water-layer test, it was observed that having thin ISMs makes the SCISEs susceptible to water-layer formation.

Keywords: Solid-contact ion-selective electrodes, high sensitivity, potentiometry, chronoamperometry, coulometric signal transduction, electrochemical impedance spectroscopy, water-layer

Preface

This master's thesis was done at Åbo Akademi University as a part of Erasmus Mundus Joint Master's Degree programme Excellence in Analytical Chemistry, under the supervision of Dr. Zekra Mousavi, senior researcher at the Laboratory of Analytical Chemistry, Åbo Akademi University.

I would like to express my sincerest gratitude to my supervisor, Dr. Zekra Mousavi for being committed and cooperative during the whole course of my laboratory work. I appreciate everything you have taught me. Many thanks to Dr. Tomasz Sokalski for all those many discussions we have had along the way. You have truly sparked my scientific mind.

To Professor Johan Bobacka, for suggesting this thesis work and guiding me through my laboratory projects. Your patience and commitment in the times of need is very much appreciated.

To Professor Ivo Leito, for being a guiding hand through the application process and for teaching us a whole load of practical analytical chemistry. Your classes will truly be missed.

To Anu, who has always been there to help me since the moment I started the programme. I will always appreciate what you have done for me.

Last, but not least, to my loved ones for being supportive and for bearing with me all this time. None of this would have been possible if you hadn't vigilantly stood by my side.

Åbo, April 2019

Nikola Obradović

Table of Contents

List of symbols and abbreviations

AC	Alternating current
a_i	Activity of species i
Ag	Silver
AgCl	Silver chloride
a_j	Activity of species j
C_{cp}	Capacitance of the conducting polymer film
C_i	Concentration of species i
C_O	Concentration of oxidized species O
D_i	Diffusion constant of species i
DC	Direct current
DOS	bis(2-ethylhexyl) sebacate
E_{cell}	Electrochemical cell potential
E_I	Potential intercept from calibration
E_{ind}	Indicator electrode potential
E_j	Liquid-junction potential
E_{ref}	Reference electrode potential
E^0	Standard potential
ECP	Electrically conducting polymer
EDOT	3,4-ethylenedioxythiophene
ETH 500	tetradodecylammonium tetrakis(4-chlorophenyl)borate
F	Faraday constant
f_i	Activity coefficient of species i
GCE	Glassy carbon electrode
HCl	Hydrochloric acid
I_p	Current density
ISE	Ion-selective electrode
ISM	Ion-selective membrane
$K^{pot}_{i,j}$	Potentiometric selectivity coefficient for primary ion i over interfering ion j
KCl	Potassium chloride
KTFPB	Potatsium tetrakis[3,5-bis(trifluoromethyl)phenyl)]borate
KTpClPB	Potassium tetrakis(4-chlorophenyl)borate
LiOAc	Lithium acetate
n	Number of electrons exchanged with the electrode during a faradaic process
NaCl	Sodium chloride
NaPSS	poly (sodium 4-styrenesulfonate)

o-NPOE	2-nitrophenyloctyl ether
4-NDP	4-nonadecyl pyridine
R	Universal gas constant
R_{cell}	Resistance of the electrochemical cell
PEDOT	Poly(3,4-ethylenedioxythiophene)
PEDOT:PSS	Poly(3,4-ethylenedioxythiophene) doped with PSS
PEDOT:Cl^-	Poly(3,4-ethylenedioxythiophene) doped with chloride
PVC	Poly(vinyl chloride)
SCISE	Solid-contact ion-selective electrode
t	Measurement time
T	Absolute temperature
TDMACl	tridodecylmethylammonium chloride
u_i	Mobility of ion i
z_i	Charge of ion i
z_j	Charge of ion j
α	Reference solution phase
β	Sample solution phase
ν	Scan rate
ϕ	Phase shift (angle)
ω	Angular frequency
s_d	Standard deviation

1. Introduction

Chemical sensors are highly sought-after devices in the modern society due to the increased need to monitor different aspects of our daily lives. Be it the monitoring of fluoride in drinking water or the glucose levels in blood, the need for sensors is apparent and is constantly growing. Working on different physico-chemical principles, the chemical sensor technology is revolutionizing the way we monitor our surroundings.[1,2,3] One of the classical types of chemical sensors are potentiometric ion-selective electrodes (ISEs), which have been employed for the determination and monitoring of ionic concentrations in a wide variety of media, from environmental to clinical.[4,5] One of the promising types of ISEs are the so-called solid-contact ISEs (SCISEs), especially those based on conducting polymers as solid contacts. Their robustness and low maintenance requirements make them very attractive both to the scientific and the general community.[6] Even though the past decade has seen an increase in the interest in ISEs and other chemical sensors, mostly due to the development of wearable and flexible chemical sensors, many issues have been raised regarding their future.[7,8]

Led by the pioneering works of Bobacka et al. in 2015, a novel signal transduction method was developed for SCISEs[9]. The method resembles the principle of constant potential coulometry and utilizes a three-electrode system in which the potential between the working electrode (solid-contact ISE) and the reference electrode is kept constant. When a change in the concentration of the analyzed ion (primary ion) occurs, the phase boundary potential of the membrane/solution interface will change and result in a redox process inside the solid contact that will proceed until the potential of the solid contact exactly matches the potential of the membrane/solution interface. While the redox process is taking place, a transient current will flow, which, when integrated with respect to time, will result in the total charge accumulated by the change in potential (as the result of the change in concentration).[9,10] The results show that the charge is linearly dependent on the logarithm of the activity of the measured primary ion. The method has proved to be useful in detecting small changes in concentration (even on the order of 0.1% change),[11] which is not possible with currently employed potentiometric techniques. But, the results have also indicated that there is a trade-off between the analysis time and the sensitivity of the method. Increasing the capacitance of the solid contact will increase the sensitivity at the cost of increased analysis time. On the other hand, the current-time profile seems to depend on the ion-selective membrane (ISM), with thinner membranes leading to higher current spikes compared with thicker membranes.[11-13]

This thesis aims to further elucidate the principles of operation of the coulometric signal transduction method and compare it with the well-known potentiometric method. Introducing a different method for preparing thin membrane SCISEs, three different SCISEs, namely potassium, hydrogen and chloride, are tested both coulometrically and potentiometrically, with the aim of elucidating what analytical benefits are obtained by employing the coulometric method. Poly(3,4-ethylenedioxythiphene) (PEDOT), doped with either polystyrene sulfonate (PSS) or chloride anions, is used as the solid contact. The coulometric behaviours of different ISEs are intercompared with the purpose of describing the influencing factors in the operation of the coulometric signal transduction method. Additionally, solid contacts without ISM are tested in the same conditions as the ISEs to further probe the influencing factors of the ion-to-electron transduction in this novel coulometric method. By employing coulometry and electrochemical impedance spectroscopy, the results obtained in this thesis can offer more clarity to the operating principles of the newly developed coulometric signal transduction method, while at the same time evaluating its performance compared to classical potentiometry method.

2. Chemical sensors

Chemical sensors are defined (by IUPAC) as devices that are able to transform a chemical information, either some specific analyte concentration or total concentration of certain species in the sample, into an analytically useful signal. One could argue that the sensing process in chemistry is nothing more but an information-acquisition routine which provides an insight into the chemical composition of the sample in real-time.[14,15] The two main parts of a chemical sensor are: chemical recognition element and transduction element (**Figure 1**). The chemical recognition element is the part of the chemical sensor which takes advantage of a chemical event (e.g. reaction), producing a signal such as colour change or a change in surface electrical potential. The transduction element serves the purpose of responding to this signal, translating its magnitude into a useful measurable signal (such as current), which in turn correlates with the amount of analyte present in the sample. It is often the case that the transducer is connected to an amplifying unit or the amplification takes place during the recognition event itself (usually the case in enzyme-based biosensors).[1,15,16]

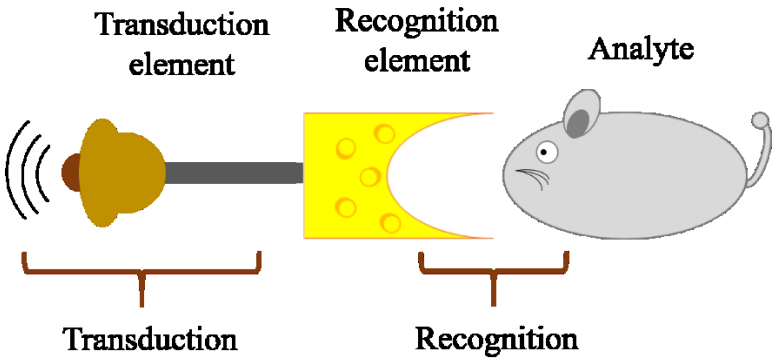

Figure 1. Schematic presentation of chemical sensor components

Depending on the mode of transduction, four different types of chemical sensors can be differentiated:[1]

- Electrochemical – based on the direct current transduction, change in potential or conductivity
- Optical – based on reflectance, absorbance or luminescence types of transduction
- Heat sensitive (calorimetric) – based on monitoring the evolved heat of reaction via thermistor couples or thermometers
- Mass sensitive (piezoelectric) – based on monitoring the frequency change of a piezoelectric crystal/surface

Chemical recognition element also serves the purpose of imparting selectivity to the sensor. Ideally, the chemical sensor would be specific for one chemical species, i.e. in a mixture of the target chemical species with interfering chemical species, the sensor would only respond to the desired one. However, in reality it can only be more selective to the desired chemical species in comparison to other, interfering chemical species. For example, one of the first constructed ISEs – the glass electrode for pH measurement shows an extremely high selectivity to hydronium ions in presence of other alkali metal ions. Following the Cremer's groundbreaking discovery, it was further discovered that the glass composition is the main factor affecting the selectivity.[17,18]

In chemical terms, the selectivity can be of two main types[15]:

- Equilibrium based selectivity, e.g. ISEs, such as glass electrode
- Kinetics based selectivity, e.g. enzyme kinetics in biosensors

3. Ion-selective electrodes

Ion-selective electrodes (ISEs) are maybe the largest subgroup of electrochemical sensors.[19-21] As mentioned previously, Cremer's ground-breaking discovery had set the path in the field of ion-selective electrode research.[18] The so-called pH electrode is arguably the most common instrument found in the laboratories and environmental analysis kits all around the world. Following Pressman's discovery of valinomycin's mechanism of action,[22] the group of Simon *et al*. has developed a liquid membrane based potassium ISEs which has set the path for a new type of ionophore based ISEs.[23] The discovery of conducting polymer films of polyacetylene had a remarkable impact on the field of ISEs,[24] as it allowed for the introduction of solid-contact electrochemical sensors led by the pioneering works of many groups around the globe.[25-28] It could be argued that the new wave of ISEs will build further upon the solid-contact ISEs and that they will remain a crucial factor in this field of research in the future.[29,30]

ISEs are one of the most common routinely used chemical sensors in the fields of clinical and environmental analysis due to their robustness and ease of use, covering the necessities for the main target ions monitored with the wide dynamic range, from 10^{-1} to 10^{-6} M, [4,5,31-38] but even lower, 10^{-11} M, detection limits have been reported.[39] There are two ISE methods that can be distinguished – indirect and direct ones.[40] The indirect methods are based on the dilution of the sample by a certain factor (1:10, 1:50…) and are most commonly used in the laboratory setting.[41] On the other hand, the direct ISE methods are the ones in which the dilution of the sample does not take place and the ISE is used for *in situ* monitoring of the ions of interest.[42] The works in developing ISEs for the latter method, such as all solid-state ISEs,[43,44] show that the community's interest in *in situ* ion monitoring has always been a driving force for ISE development.[45]

4. Poly(vinyl chloride) (PVC) based ion-selective membranes

The recognition element of the potentiometric sensor, i.e. ISE, is the ion-selective membrane (ISM). Among different types of ISMs, PVC based ISMs are the dominant ones due to the possibility of incorporating different ionophores, flexibility of the prepared ISM and the ease of preparation, as it requires no special equipment nor additional heat and pressure to be applied[46,47]. The PVC based ISMs most commonly contain four components – plasticizer, PVC, ionophore and/or lipophilic salt.[48,49]

The ionophore, which can be charged or neutral, such as macrocyclic compound valinomycin, is responsible for the selective extraction of the target ion, leading to the creation of phase boundary potential which is measured against the reference electrode. It should be noted that for the sake of simplicity the diffusion potential within the membrane is ignored. The ionophores are chosen by their ability to selectively bind a target ion due to their physico-chemical properties and complementary interactions with the target ion (van der Waals interactions, size exclusion and ionic interactions). Such ionophores, also used in this work, are shown in **Figure 2**. It should be noted that the more complementary interactions can be formed between the ionophore and the target ion, the better is the ISE able to differentiate between the primary ion and interfering ions.[48,50] Ionophores used in this work for the preparation of potassium ion-selective electrodes (K^+ ISEs) and hydrogen ion-selective electrodes (H^+ ISEs), are shown in **Figure 2a and b, respectively**. In the case of chloride ion-selective electrodes (Cl^- ISEs) studied in this work, the ion-exchanger tridodecylmethylammonium chloride was used as the ion-sensitive compound (**Figure 2c**).

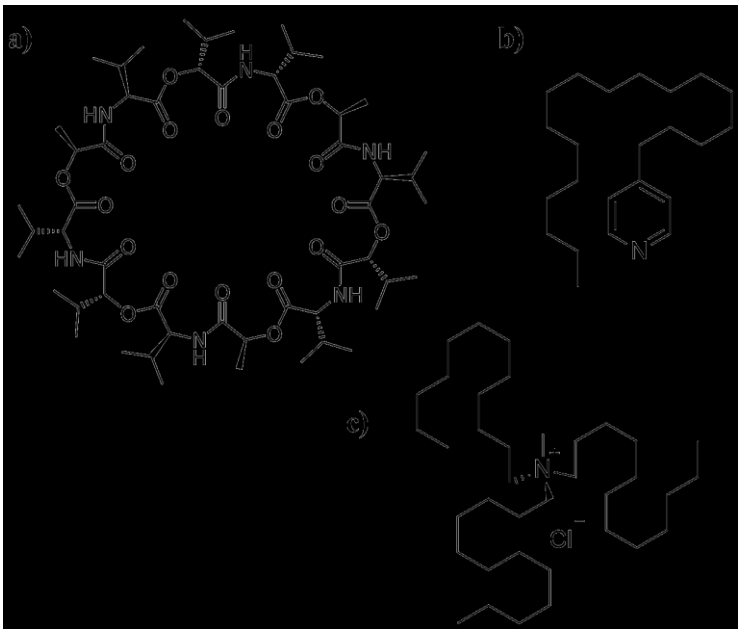

Figure 2. Structures of the ionophores used in this study: a) valinomycin in K^+ ISEs, and b) 4-nonadecylpyridine in H^+ ISEs; and c) the ion-exchanger tridodecylmethylammonium chloride used in Cl^- ISEs.

The high molecular weight PVC makes the ISM essentially hydrophobic, preventing the leakage of other hydrophobic components from the membrane, such as the plasticizer, ionophore and/or lipophilic salts.[48] The plasticizer gives the ISM liquid phase properties, enabling the ion-exchange to take place through the membrane. The plasticizer is responsible for the ISM's flexibility as an important mechanical feature, while also controlling the ISM's

dielectric properties and hydrophobicity.[15,48] The most common plasticizers used in the preparation of ISMs are shown in **Figure 3**.

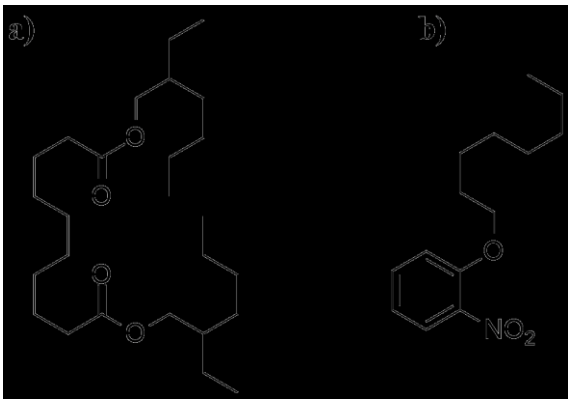

Figure 3. Commonly used plasticizers: a) bis(2-ethylhexyl)sebacate (DOS) and b) 2-nitrophenyl octyl ether (o-NPOE)

The lipophilic salts (a.k.a. ionic sites) are used in ISMs for several purposes. They reduce the effect of interference from the lipophilic ions in the sample and counter ions, also known as permselectivity or Donnan exclusion. The presence of lipophilic salts is beneficial as they significantly reduce the electrical resistance of the ISM and are able to increase the sensitivity of ISEs with ionophores of poor extraction capability. However, the ratio of the lipophilic salt to ionophore in the ISM must be strictly controlled, as an excess of lipophilic salt would dramatically influence the selectivity of the membrane, making it nothing more but a common ion-exchanger.[51-53] Some examples of lipophilic salts are shown in **Figure 4**.

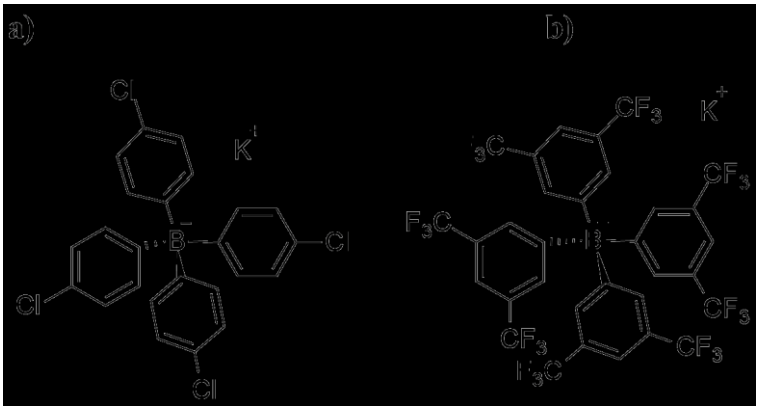

Figure 4. Commonly used lipophilic salts: a) potassium tetrakis(4-chlorophenyl)borate and b) potassium tetrakis[3,5-bis(trifluoromethyl)phenyl)]borate

PVC based ISMs most commonly have the following composition by weight – 60-66% of the plasticizer, 30-33% of PVC and 0.5-3% ionophore plus the lipophilic salt. As previously mentioned, the ionophore-to-lipophilic salt ratio needs to be carefully optimized (usually 50 mol% of the ionophore content) in order to obtain the desired selectivity. In the case of SCISEs,

the membrane components are dissolved in a suitable solvent, most commonly tetrahydrofuran (THF), and are drop-casted or spin-coated onto the electrode surface. After being left to dry for 1-2 day, the electrode is conditioned in an appropriate solution, after which it is ready for use.[48,51,54,55]

5. Electrically conducting polymers as potentiometric transducers

Electrically conducting polymers (ECPs) used in SCISE technology are carbon-based materials containing polyene structure, i.e. alternating single and double bonds (**Figure 5**). This single-double bond alternation is also called conjugation or π-conjugation, so a term conjugated (π-conjugated) polymers is also used. In their pristine state, conjugated polymers behave either as insulators or as semiconductors. Only after the doping process do they gain electrically conducting properties of common ECPs, on the scale of tens to hundreds of Siemens per cm.[56,57]

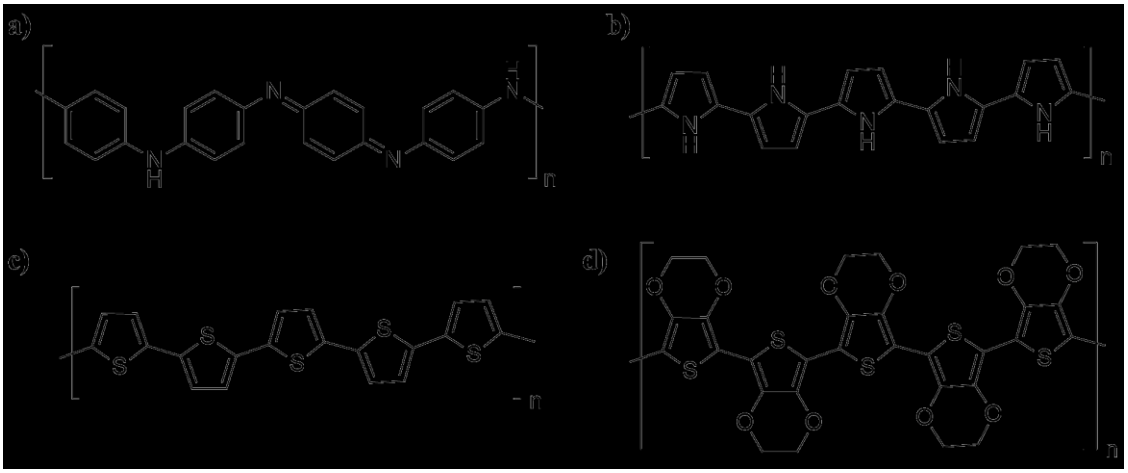

Figure 5. Molecular structures of common ECPs: a) polyaniline, b) polypyrrole, c) polythiophene, d) poly(3,4-ethylenedioxythiophene), also known as PEDOT

Two different approaches to ECP synthesis have been employed so far – chemical and electrochemical. Chemical polymerization of ECPs is usually recommended if large quantities of polymer are needed. The reaction usually requires the use of a catalyst (e.g. Ziegler-Natta catalysts) and the polymer is obtained in an oxidized state with high electrical conductivity.[58-60]

On the other hand, the electrochemical polymerization is of significant interest application-wise, as it only requires the use of cheap monomers (such as heteroaromatic compounds in the case of PEDOT materials) and suitable electrode surfaces, such as platinum or glassy carbon.[59,60] Electrochemical polymerization are usually oxidative polymerizations, which are

performed galvanostatically, potentiostatically or potentiodynamically. In galvanostatic polymerization methods, a constant current is applied between the working and the counter electrode immersed in the polymerization solution. The polymerization time, together with the current used, will define the thickness of the formed polymer film. Alternatively, potentiostatic techniques can also be employed, in which a constant oxidative potential is applied, high enough for the polymerization to take place, but low enough to avoid any unwanted secondary reactions at the electrode surface.[59] Alternatively, potentiodynamic polymerizations can also be used, such as in the case of polyaniline synthesis. A varying potential (as in cyclic voltammetry) is applied to the working electrode in a three electrode system for a certain number of cycles.[61] The electrochemical polymerization is the main synthesis route if the obtained polymer is intended to be used in polymer film electrodes or as thin-layer sensors. The control of parameters in galvanostatic and potentiodynamic polymerizations enables the formation of a polymer film of defined and reproducible thickness and physico-chemical properties.[59,60]

As previously mentioned, the electrically conducting properties of ECPs come from the doping, which can be either of chemical or electrochemical nature. Given that this text only deals with the electrochemically synthesized ECPs, only the latter one will be shown in the **Equations 1** (p-doping) **and 2** (n-doping). It should be noted that the electrochemically synthesized polymers often get doped during the polymerization process.

$$CP_{(film)} + A^- \rightleftarrows CP^+A^-_{(film)} + e^- \qquad \text{Equation 1}$$

$$CP_{(film)} + e^- + M^+ \rightleftarrows CP^-M^+_{(film)} \qquad \text{Equation 2}$$

Where CP is the conducting polymer denoted in the subscript as film on the surface of the electrode, while M^+ and A^- are positively and negatively charged counterions, respectively. Depending on the applied potential or current, the polymer can be p-doped (oxidized) or n-doped (reduced). Both of these processes are followed by insertion of charge-compensating counterions from the solution into the formed polymer film. The reversibility of oxidation/reduction processes in conducting polymers is responsible for their use in potentiometric sensors (ISEs) as ion-to-electron transducers, as shown in chapter 8 in the example of PEDOT.[62,63]

Poly(3,4-ethylenedioxythiphoene), or commonly known as PEDOT, is an extensively studied polymer material and one with the highest efficiency among the conducting organic-based thermoelectric materials.[62,64] It's characterized by a rather high stability, giving rise to its

applications in the fields of capacitors, biosensors and all-solid-state ISEs.[63] Although it can be synthesized both chemically and electrochemically, only the electrochemical synthesis is of interest in this work. The synthesis is done galvanostatically and the polymer is obtained in a doped, oxidized form. Depending on the ions present in the polymerization solution, the polymer film will also incorporate counterions, such as small and mobile chloride ions or large, immobile polymeric ions, such as polystyrene sulfonate, resulting in an electroactive and highly stable ECP.[63,65] Depending on the ion incorporated, the PEDOT layer will show either anionic (in case of PEDOT:Cl^-) or cationic (in case of PEDOT:PSS) response.[66]

6. SCISEs based on conducting polymers

The main drawback of conventional ISEs (**Figure 6a**) is due to the liquid inner compartment. Even though conventional ISEs are most commonly found on the market today, they do not offer as wide range of possibilities for *in situ* analyses as the SCISEs.[67] Apart from that, the handling of a conventional ISE with liquid inner compartment requires complete contact of the inner compartment solution with the PVC ISM, something that is difficult to realize during *in situ* clinical or environmental measurements when the electrode needs to be used in an upside-down position. Their fragile glass bodies require careful handling, while the inner compartment solution is prone to evaporation and contamination, limiting in the same time the use of these sensors at high pressures and temperatures for prolonged periods. Another limitation that has emerged over the years is the inability of miniaturization of ISEs with inner liquid compartment, usually requiring an external reference electrode with a porous junction.[54,67-72]

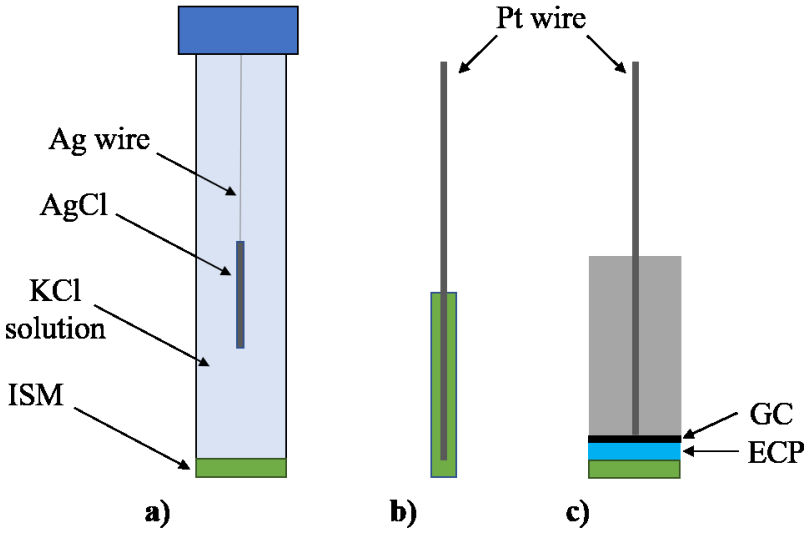

Figure 6. a) Conventional (potassium selective), b) coated-wire and c) solid-contact ISEs

The emergence of the coated-wire electrode in 1971 was the first step towards an ISE without the liquid inner compartment. The blocked charge transfer between the electronic conductor and the ISM (**Figure 6b**), in itself an ionic conductor, resulted in poor long-term potential stability and reproducibility of the response of coated-wire electrodes. The charge transfer in coated wire electrodes still remains an open subject, although some suggestions were made about oxygen playing the role of the ion-to-electron transducing species.[1,54,66,73,74]

In order to stabilize the interfacial potential, a proper ion-to-electron transducer had to be introduced between the electronic transducer and the ISM (ionic transducer). One of these ion-to-electron transducers which proved to be beneficial in the future construction of ISEs, were electrically conducting polymers (ECPs). Their ability to form ohmic contacts with materials with high work functions, such as platinum or glassy carbon (GC) and the ease of their electrodeposition onto the electrode surface made them ideal for this kind of application. Furthermore, the use of ECPs was beneficial as the ion-to-electron transduction requires mixed electronic and ionic conductivity, meaning that the ECPs can transduce an ionic signal from the ISM to an electronic signal in the solid state of the electronic transducer.[6,28,60,75] Having a PVC based ISM, as previously described, is a common way to impart ion selectivity to SCISEs based on conducting polymers as ion-to-electron transducers.[76,77]

7. Principles of measurements of potentiometric ISEs

The measurements using ISEs are based on the well-established principles of potentiometry, as indicated in **Figure 7**. The ISEs, also known as the indicator electrode, is connected to a potentiometer, alongside a reference electrode. Since the potential of the indicator electrode cannot be directly measured, the reference electrode is used as a constant potential element. The potentiometer needs to be very sensitive and to have a high input impedance, as potentiometry presents an equilibrium method which allows only for very small currents (on the order of femtoamps) to pass. Drawing higher currents from the circuit would disturb the chemical equilibrium and lead to a change in the chemical composition of the sample solution due to the reactions that would take place at the electrode surfaces.[15,48,78]

The most common reference electrodes (silver/silver chloride and calomel electrodes) consist of a metal covered with a sparsely soluble salt of that metal and immersed into the solution containing the common anion of that salt in high concentration. This type of reference electrode construction helps maintain the reference electrode's potential constant, as the composition of

the electrode and the surrounding solution will not change during the ion-to-electron transduction in low current regime of potentiometry.

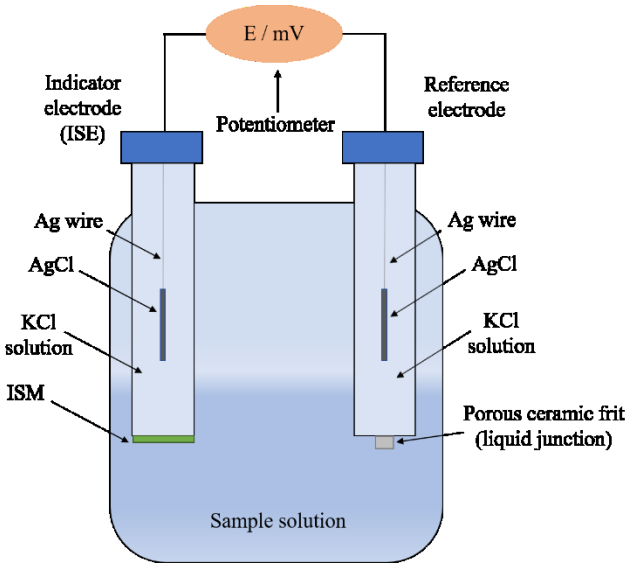

Figure 7. A schematic representation of the set-up for potentiometric measurements using conventional potassium ISE

The magnitude of the potential arising from the interaction of the ISM with the target ion in the solution via ion-exchange is given by the following equation:

$$E_{cell}=E_{ind}-E_{ref}+E_j \qquad \text{Equation 3}$$

Where E_{cell} (also known as electromotive force, EMF) is the potential difference measured in the electrochemical cell, E_{ind} is the potential of the indicator electrode (ISE), E_{ref} is the potential of the reference electrode and E_j is the liquid junction potential. The liquid-junction potential develops across the phase boundary of two dissimilar solutions, which is the case with the reference electrode's internal filling solution and the solution being analysed. Apart from the difference in ion concentration, the liquid-junction potential is also dependent on the ionic mobility, and is usually estimated by the Henderson equation:[78]

$$E_j=\frac{\sum_i \frac{|z_i|u_i}{z_i}[C_i(\beta)-C_i(\alpha)]}{\sum_i|z_i|u_i[C_i(\beta)-C_i(\alpha)]}\frac{RT}{F}\ln\frac{\sum_i|z_i|u_iC_i(\alpha)}{\sum_i|z_i|u_iC_i(\beta)} \qquad \text{Equation 4}$$

Where z_i is the charge of the ionic species i, u_i is the mobility of the respective ion and C_i the concentration of the respective ion, α and β are used to denominate the internal reference solution and the sample solution phases. Liquid-junction potential is the most common artifact in potentiometric measurements and an effort is made to keep it low and approximately constant by using an internal reference solution of high salt concentration, with cations and anions being of as equal mobility as possible.

The electrochemical cell potential established between the indicator ISE and the reference electrode immersed in the same solution is linearly correlated to the logarithm of the activity of the target ion (the ion to which the membrane is selective), as given by the Nernst equation:[79,80]

$$E=E^{0}+\frac{RT}{z_{i}F}\ln a_{i} \qquad \text{Equation 5}$$

Where E is the measured potential, $E^{0'}$ is the standard (or formal) potential which includes all of the electrochemical cell characteristics, R is the universal gas constant, T the absolute temperature in Kelvin, z_i the charge of the primary ion, F the Faraday constant and a_i the activity of the primary ion. At room temperature of 25°C (298.15 K), the slope of the calibration curve for monovalent cationic responsive ISE would be 59.16 mV, while the slope of the calibration curve for monovalent anionic responsive ISE would be -59.16 mV, as shown in **Figure 8**.

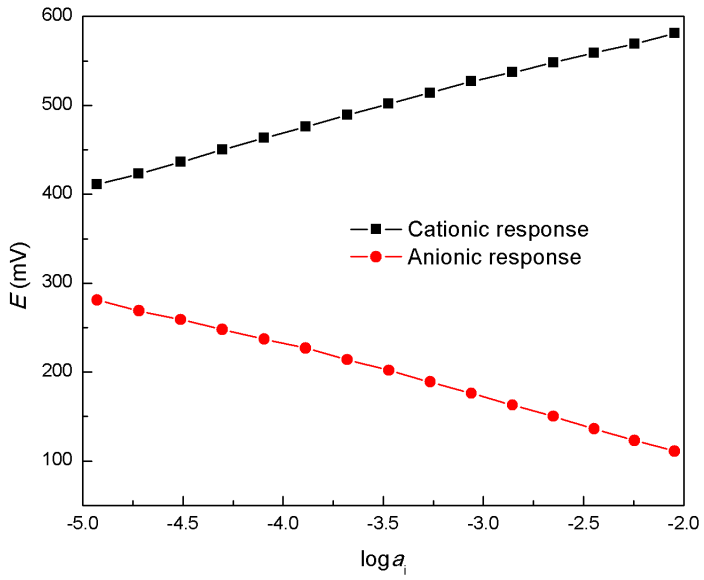

Figure 8. Typical calibration curves for cationic and anionic responsive ISEs

The selectivity of the ISEs is described by the selectivity coefficient, featured in the Nikolskii-Eisenman equation:[81, 82]

$$E=E_{I}+\frac{59.16\ \text{mV}}{z_{i}}\log\left(a_{i}+\sum_{i\neq j}^{j}K_{i,j}^{pot}a_{j}^{\frac{z_{i}}{z_{j}}}\right) \qquad \text{Equation 6}$$

Where E is the measured potential difference, E_I is the intercept obtained from the calibration curve, which includes all constant potential components, z_i and z_j are the charges of the primary and interfering ions, respectively and a_i and a_j are the activities of the primary and interfering ions, respectively. The $K_{i,j}^{pot}$ is a quantitative parameter describing the extent to which the ISE is responsive to the target (primary) ion in the presence of an interfering ion. For example, if the value of $K_{i,j}^{pot}$ is equal to 0.01 for ions i and j which are of the same charge then the ISE is one hundred times more responsive towards the primary ion compared to the interfering ion. According to the Nikolskii-Eisenman equation, the interfering ionic species will affect the response of the ISE only when the term $\sum_{i\neq j}^{j} K_{i,j}^{pot} a_j^{\frac{z_i}{z_j}}$ is of comparable magnitude as a_i. This is mainly noticeable near the detection limits of ISE methods, which are mainly influenced by the electrode's selectivity towards the interfering ionic species in the analysed sample solution.[48,78,79-82]

8. Principles of measurements in novel coulometric transduction-based ISEs

Up until the 21st century, the ISEs, both conventional and SCISEs, were generally used in the potentiometric transduction regime. As was previously described, this method is based on measuring the equilibrium potential of the electrochemical cell, consisting of two electrodes, the indicator (ISE) and the reference electrode.[15,48,78] The use of potentiometric ISEs still requires calibration prior to its application and the methods, both direct and indirect, have not undergone significant changes.[40] That was all until a new coulometric ion-to-electron signal transduction method had emerged in 2015, led by the pioneering works of Bobacka et al.[9] This novel method utilizes the previously described SCISEs, but in a different setup than potentiometry. The method is based on constant potential coulometry, utilizing a common three-electrode system with a constant potential being held between the working (SCISE) and reference electrodes. In a coulometry-based ISE setup, shown in **Figure 9**, a change in the concentration of the primary ion (1) leads to a change in the interfacial membrane/solution potential (2) and thus to a rise in potential difference between the working and reference electrodes. Due to the arisen potential difference, a transient current will flow through the working and counter electrodes until a new equilibrium is reached (3). The flow of current will utilize the redox capacitance of the conducting polymer, making it undergo oxidation or reduction (**Equation 7**) until the change in potential of the conducting polymer compensates

for the interfacial membrane/solution potential difference (4). Upon complete compensation, the current will cease to flow and the obtained current-time profile can be integrated to obtain the charge (5).[9-13]

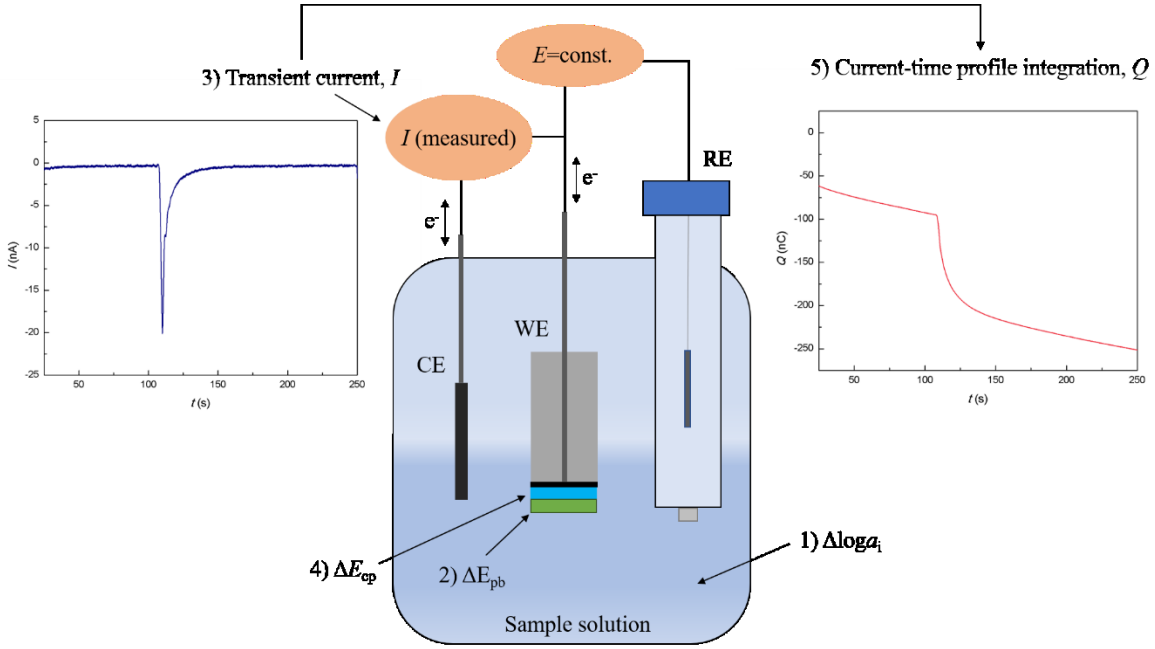

Figure 9. The principle of operation of coulometric signal transduction. ΔE_{pb} is the change in the phase boundary potential, while ΔE_{cp} is the change in the potential of the ECP

$$PEDOT^{+}PSS^{-}_{(film)} + M^{+} + e^{-} \rightleftarrows PEDOT^{0}PSS^{-}M^{+}_{(film)} \qquad \text{Equation 7}$$

Since the proof of concept of this method has been introduced in 2015,[9] several papers followed offering a theoretical model of the operation of this method,[13] together with practical applications in different types of samples, such as seawater and human serum.[11] Despite the fact that it requires at least one point calibration, the method is promising to revolutionize the field of ion sensors and bring the society a step closer to calibration-free SCISEs.[9] So far, the results have shown that the coulometric signal transduction method makes it possible to use the common framework of ISE calibration, showing a linear dependence of the signal (charge) to the logarithm of ionic activity.[11,12]

As can be seen in **Figure 9**, the current transient profile is concordant with the potential change at the membrane/solution interface and the surge of primary ions to and from the ISE when a change in concentration has been performed. The sudden surge of ions causes a high current to flow, which diminishes in time with a time constant equal to the product of R_{cell} and C_{cp}, as shown by the equation below:[13]

$$I = \frac{59.16\ \text{mV}}{z_i R_{cell}} \log\left[\frac{a_i(\text{initial})}{a_i(\text{final})}\right] e^{\frac{t-t_0}{R_{cell}C_{cp}}} \qquad \text{Equation 8}$$

where R_{cell} is the electrochemical cell resistance, mainly influenced by the resistance of the ISM and C_{cp} is the capacitance of the ECP, z_i is the charge of the primary ion, a_i its respective activity, t_0 is the time of the change in activity of the primary ion, while t is the time elapsed during the measurement. The equilibration time (the time when the current level converges to zero) has proved to be rather long, because as the current driving force (ΔE_{pb}) diminishes, so does the redox process shown in **Equation 7** slow down. Furthermore, it shows that the time constant, $R_{cell}C_{cp}$, can be adjusted by varying the R_{cell} and C_{cp}.[10,12,13]

The results have shown that in order to reduce the equilibration time of the current-time profile, the thickness of both the ECP and the ISM should be reduced.[10,12] For electrodes of constant ECP and ISM thickness, increasing the electrode's surface diameter has proved to be beneficial in increasing the current transient, most probably due to the better utilization of the redox capacitance of the ECP that is spread across a larger surface area. The results have clearly shown that the concentration change and the electrode's resistance play the biggest role in the height of the measured current (right after the concentration change), while the redox processes occurring in the bulk of ECP, together with the ionic mass-transport, play the biggest role in the later stages of equilibration.[10]

One way of utilizing the electrode's redox capacitance is tuning (amplifying) the sensitivity of the proposed ion-to-electron signal transduction method. The results show that having a thicker ECP (higher redox capacitance) leads to broader current-time transient peaks, i.e. larger values of charge obtained upon integration. This observation is in agreement with the assumption that the oxidized-to-reduced PEDOT ratio in the ECP is constant at a certain potential, regardless of the ECP thickness. Upon the potential change, as previously described, the ECP undergoes a redox change, with thicker ECPs having more material to be oxidized/reduced, leading to higher current signals and consequently higher integrated charges. Unfortunately, this will also result in longer equilibration times, so a trade off has to be made between the time of the analysis and the method's sensitivity. Since the amount of obtained charge is higher for bigger changes in the primary ion's activity, thicker ECPs would be most suitable in those types of analyses that would require small changes in the activity to be monitored.[12]

The resistance of the ISM was also considered in the previous works of Han et al., where the membrane's resistance is decreased by adding salts with both lipophilic cations and anions

(like ETH 500) and by decreasing the thickness of the membrane by spin-coating procedure leads to lower equilibration times and higher measured current spikes, i.e. narrower current-time profiles.[10-13]

9. Characterization techniques

9. 1. Cyclic voltammetry

Cyclic voltammetry (CV) is an extension to linear sweep voltammetry in which the potential is first swept to a certain value and then swept back to the original value (**Figure 10**). It is based on the commonly known three-electrode system in which the potential is changed between the working and the reference electrodes, while the current flowing between the working and the counter electrodes is measured. The experiments are performed in an unstirred solution. Cyclic voltammetry is most commonly used for the qualitative study of electrochemical systems as it gives information about the half-wave potentials and electron-transfer kinetics.

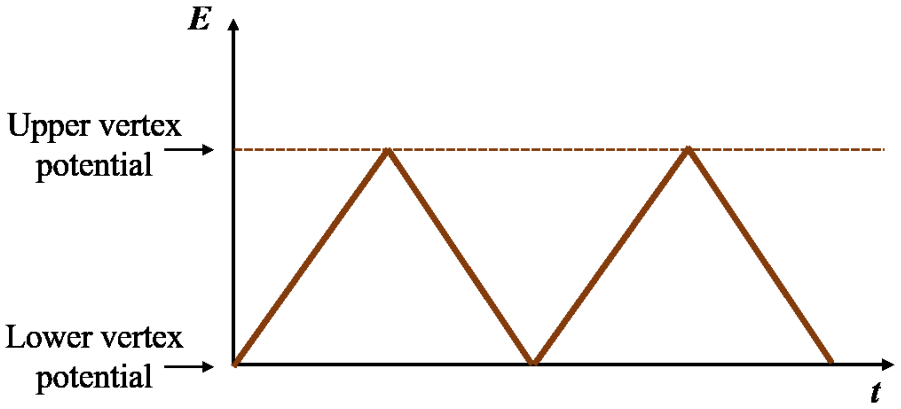

Figure 10. Potential vs. time plot of cyclic voltammetry measurements

There are often many peaks in the cyclic voltammograms, which can be influenced by changing the initial and ending potentials or scan rate. The resulting peaks, with their current dependence on the scan rate, as well as with their potential difference offer insights into how an electrochemical system behaves – number of electrons transferred, reversibility of the electrochemical system, identification of adsorption, as well as of coupled chemical reactions. The current in cyclic voltammetry is given by the Randles-Sevčik equation:

$$I_p = -\left(2.69\times10^5\right) n^{3/2} C_O D^{1/2} \nu^{1/2} \qquad \text{Equation 9}$$

Where I_p is the current density (A/cm^2), n is the number of electrons exchanged with the electrode during the reaction, C_O is the concentration of the oxidized form of the electroactive

species in the solution (mol/cm^3), D (cm^2/s) is the diffusion coefficient and ν is the potential scan rate (V/s).[83]

As previously mentioned, cyclic voltammetry can e.g. be used for electropolymerization of aniline and ECP characterization.[61] The latter, together with checking the polishing results of the electrodes, was the reason for using cyclic voltammetry in this thesis.

9. 2. Potentiometry

Potentiometry is one of the classical electrochemical techniques, where the information about the sample is obtained by measuring the potential difference between two electrodes. The classical electrochemical cell for potentiometric measurements is comprised of two electrodes, indicator and reference, immersed into the studied solution and connected through a potential measuring device – potentiometer. The potentiometer needs to have a high input impedance as to allow for minute currents to flow (in the order of magnitude of pA-fA), as the measurement mode in potentiometry is that of an equilibrium, which would be disturbed if significant currents were allowed to pass through the cell. In the case of ISEs, the reference electrode, as described previously, is used as a constant potential element, allowing for a correlation to be made between the measured potential difference and the logarithm of activity of the target ion, as shown in the Nernst equation (**Equation 5**).[15, 48, 78] According to the Nernst equation, the ISEs are responsive to ionic activities, rather than concentrations. Activities denote the "active" concentration of the ionic species in the solution and are calculated from the concentrations using the following equation:

$$a=f_i c_i \qquad \text{Equation 10}$$

Where f_i is the activity coefficient and c_i the concentration of the respective ionic species. The activity coefficient is dependent on the ionic strength of the solution, as well as on the type of the ions (most importantly in terms of charge and ionic radius). The activity coefficient can be calculated using the Debye-Hückel equation.[84] In this thesis, potentiometry was used for the characterization of prepared ISEs, mainly in terms of measuring their sensitivities and, also, for checking the potential stability of ISEs with time, most importantly during the water-layer test experiment. Additionally, for the sake of comparison with chronoamperometry/chronocoulometry, potentiometry was employed in the standard addition/dilution experiments.

9. 3. Chronoamperometry and chronocoulometry

While the previously described cyclic voltammetry was based on measuring the current during a constant and defined change in potential,[83] chronoamperometry is based on measuring the current in the same three-electrode setup but at a constant potential (or sudden changes in potential) for a certain amount of time. Besides being utilized in glucose biosensors,[85] chronoamperometry is also used for determining diffusion constants, rates of electrode reactions, both simple and coupled with chemical reactions, and adsorption parameters.[86,87] Charging of the double layer, i.e. the capacitive changes, is responsible for the current spike in the chronoamperometric measurements, a process similar to the one described in the novel coulometric signal transduction method.[10-13]

Chronocoulometry is nothing more than an integral of the chronoamperometric signal. Also known as constant-potential coulometry, it offers the information of the charge that's passed through the electrochemical system. As it is obtained by computational methods, chronocoulometry has also proved to eliminate noisy baselines seen in chronoamperometry.[11]

In this thesis, chronoamperometry and chronocoulometry were used for characterizing the behaviour of the SCISEs in the newly proposed coulometric signal transduction method via standard addition/dilution experiments.

9. 4. Electrochemical impedance spectroscopy (EIS)

While the concept of resistance is quite common and familiar from the study of direct current (DC) circuits, for the alternating current (AC) circuits the concept of impedance is used. It is equal to the potential/current ratio of an AC circuit. When a small amplitude sinusoidal (AC) excitation potential is superimposed on a fixed DC potential, a sinusoidal alternating current is measured with an appropriate angular frequency (ω) and a phase shift (ϕ, phase angle) between the applied excitation potential and the resulting current response.[78,88]

$$E(\omega)=E_0 \sin(\omega t) \qquad \text{Equation 11}$$

$$I(\omega)=I_0 \sin(\omega t+\phi) \qquad \text{Equation 12}$$

Where E_0 and I_0 are the corresponding potential and current amplitudes, respectively. Values of phase shifts can give an insight into the behaviour of the given electrochemical system, where 0° would correspond to a resistor, 45° corresponds to Warburg impedance (further described below) and 90° corresponds to a capacitor.

The system's impedance is given as a vector, with magnitude $|Z|$, consisting of a real impedance component (Z') and an imaginary impedance component (Z''), shown in **Figure 11**. After collecting the impedances at different frequencies, the "heads" of all obtained vectors are plotted into the so-called Nyquist plot.

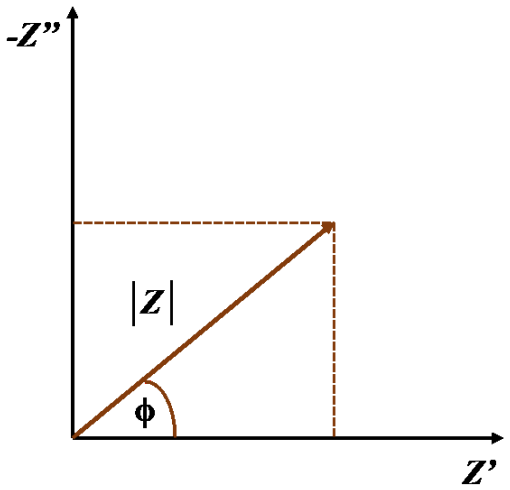

Figure 11. Nyquist plot of an impedance vector

Nyquist plots, as the simple one shown in **Figure 11** or the ones shown further in this thesis, are plots of the imaginary impedance component vs. the real impedance component, with no information about the value of the applied AC frequency to which the points in the plot corresponds. They can help in explaining the electrochemical process occurring at the electrode surface. This is primarily done via using the so-called equivalent circuits. An equivalent circuit is an electrical circuit representation of the processes which are going on in the system under study. It is a bridge between the real physical phenomena going on in the studied electrochemical system and their theoretical representation and explanation. For example, a system in which a charge transfer is occurring at an electrode in contact with an electrolyte solution can be broken down into its electrical constituents, e.g. the resistance of the solution, the capacitance of the double layer forming on the electrode-solution interface, the resistance of charge-transfer at the electrode surface, the charge diffusion from and towards the electrode, etc. With all of this information, one can use the data obtained from EIS measurements to model an equivalent circuit and,*vice versa,* to explain the physico-chemical processes with an equivalent circuit model.

The "simplest" equivalent circuit describing the above-mentioned electrochemical processes in an electrochemical system is the Randle's circuit. It is a circuit that models the system in which a redox (faradaic) process occurs. According to the Randle's circuit (**Figure 12**), one

can model the system as a resistor (coming from the resistance of the electrolyte solution, R_s) in series with the impedance component consisting of a faradaic impedance (due to the charge-transfer resistance, R_{ct}, and Warburg impedance, Z_W, which arises from the diffusion of the redox species to and from the electrode) in parallel with the double layer capacitance, C_{dl}.[78,83,88]

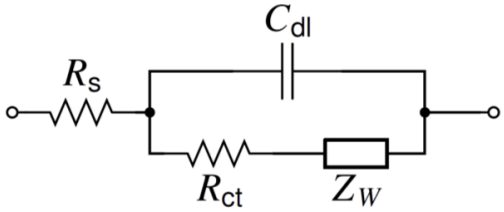

Figure 12. Randle's circuit

Electrochemical impedance spectroscopy enables one to obtain information about the electrochemical system in the frequency domain – more accurately, the signal (impedance, phase shift) of the system with respect to the frequency of the applied perturbation potential. Differently from other electrochemical methods, such as potentiometry or voltammetry, EIS can be used to investigate the electrochemical systems in a wide frequency range (10^{-5}-10^{7} Hz) and low signal output. This is especially the case with fast processes in which diffusion can become the rate determining process instead of the kinetics one wants to study at the electrode surface. It can be widely used for the characterization of conducting polymers and different electrode coatings, for probing the energy storage for batteries and fuel-cells and, also, for the studies of electrochemical kinetics and adsorption processes at the electrode/solution interface. Differently from other electrochemical techniques, EIS allows for a more detailed characterization of complex systems (such as multiple electrode coatings, e.g. conducting polymers with different membranes on top of them).

In this thesis, EIS was used to characterize the electrochemical behaviour of the prepared SCISEs in order to get a further insight into the mechanism of operation of the coulometric signal transduction method.

10. Experimental

10. 1. Materials

3,4-ethylenedioxythiophene (EDOT, 97%), poly(sodium 4-styrenesulfonate) (NaPSS; MW≈70.000), potassium chloride (KCl, ≥99.5%) and sodium schloride (NaCl, ≥99%) were obtained from Sigma-Aldrich. Poly(vinyl chloride) (PVC), of high molecular weight, potassium ionophore I (valinomycin), hydrogen ionophore I (4-nonadecyl pyridine, 4-NDP),

potassium tetrakis(4-chlorophenyl)borate (KTpClPB), potatsium tetrakis[3,5-bis(trifluoromethyl)phenyl)]borate (KTFPB), 2-nitrophenyloctyl ether (o-NPOE), bis(2-ethylhexyl) sebacate (DOS), tetradodecylammonium tetrakis(4-chlorophenyl)borate (ETH 500), tridodecylmethylammonium chloride (TDMACl), and tetrahydrofuran (THF, >99.9%) were obtained from Fluka (Selectophore Grade Reagents), as well as the hydrochloric acid (HCl, ≥37%). Distilled and deionized water (ELGA Purelab Ultra; resistivity 18.2 MΩcm) was used in preparing the solutions for all of the experiments. The standard buffer solution of pH=7.00 was obtained from ThermoScientific.

All of the cyclic voltammetry and electropolymerization experiments were performed in a three-electrode electrochemical cell connected to Autolab General Purpose Electrochemical System (AUTO30.FRA2-Autolab Eco Chemie, B.V., The Netherlands).

All of the potentiometric experiments were carried out using a two-electrode electrochemical cell connected to 16-channel millivoltmeter (Lawson Labs. Inc., Malvern, PA, USA).

All of the chronoamperometry/chronocoulometry and electrochemical impedance spectroscopy experiments were carried out using IviumCompactStat (Ivium Technologies, The Netherlands).

10. 2. Ion-selective membrane cocktail preparation

The substances needed for cocktail preparation were weighed together in a 10 mL glass vial. The mixture was vortexed until all of the compounds seemed completely dissolved. The vial was wrapped with Al foil and left on a rocker overnight to slowly shake to allow for complete dissolution of PVC. The ISM cocktails were stored in the fridge (4°C) before use. All cocktails had the final dry mass content of 15%, determined as the ratio of the sum of all ISM components masses (excluding THF) to the sum of all components' masses including THF.

Table 1. The composition of ion-selective membrane cocktails

Potassium			Hydrogen			Chloride		
Substance	m (mg)	ω (%)	Substance	m (mg)	ω (%)	Substance	m (mg)	ω (%)
Valinomycin	2.00	1.00	4-NDP	2.01	1.00	TDMACl	29.99	14.99
KTFPB	1.00	0.50	KTpClPB	2.02	1.00	o-NPOE	102.05	51.01
ETH 500	2.04	1.02	o-NPOE	136.09	68.00	PVC	68.02	34.00
DOS	130.10	64.93	PVC	60.00	29.98	THF	1134.1	-
PVC	65.24	32.56	THF	1134.3	-	-	-	-
THF	1134.0	-	-	-	-	-	-	-

10. 3. Electrode preparation

Glassy carbon disk electrodes (GCEs), mounted in PVC cylinders were used for the preparation of ISEs in this work, while GCEs mounted in polyether ether ketone (PEEK) cylinders were used for the preparation of electrodes without ISM. The diameter of the glassy carbon substrate that was used is 3 mm, corresponding to the electrode area of 0.071 cm^2. The electrodes were prepared for use by polishing in the following manner (sequentially, from top to bottom, left to right):

Table 2. Electrode polishing scheme

Polishing medium	Polishing time	Polishing medium	Polishing time
Sandpaper 180	1 min	Diamond Paste 9 µm	1 min
Sandpaper 600	1 min	Diamond Paste 3 µm	1 min
Sandpaper 1000	1 min	Diamond Paste 1 µm	1 min
Sandpaper 2000	1 min	Alumina Slurry 0.3 µm	1 min
Sandpaper 2500	1 min	Alumina Slurry 0.05 µm	1 min
Diamond Paste 15 µm	1 min	Clean cloth	1 min

After polishing, the electrodes were ultrasonicated in ethanol and deionized water for 15 min, respectively.

10. 4. Galvanostatic polymerization

The galvanostatic synthesis of PEDOT:PSS and PEDOT:Cl^- was done as described in the previous papers of Bobacka et al.[10, 11, 13] and carried out using a three-electrode electrochemical cell connected to an Autolab General Purpose Electrochemical System (AUTO30.FRA2-Autolab Eco Chemie, B.V., The Netherlands). The working electrode was the previously mentioned GCE (area 0.071 cm^2), the auxiliary electrode was a GC rod and the reference electrode depended on the polymer to be synthesized. In the case of PEDOT:PSS, a Metrohm double junction electrode Ag/AgCl/3 M KCl/0.1 M NaPSS was used, while in the case of PEDOT:Cl^- a Metrohm single junction electrode Ag/AgCl/3 M KCl was used. Galvanostatic polymerization of EDOT:PSS was performed in a deaerated (by purging for 15 minutes with N_2) solution of 0.01 M EDOT+0.1 M NaPSS as supporting electrolyte, while the polymerization of EDOT:Cl^- required a dearated solution of 0.01 M EDOT+0.1 M KCl. A constant current of 0.0141 mA was applied between the working and the counter electrodes for 142 s to obtain the polymerization charge of 2 mC. After polymerization, the electrodes (GCE/PEDOT:PSS and GCE/PEDOT:Cl^-) were thoroughly rinsed with deionized water and left to condition in 0.01 M KCl (in case of potassium and chloride ISEs) or 0.01 M HCl (in case of hydrogen ISEs) for at least 24 hours. Thereafter the electrodes would either be

calibrated and further used in electrochemical experiments or left to dry for at least 24 hours before applying the ISM cocktail.

10. 5. Potassium, hydrogen and chloride SCISE preparation

The described procedure was adopted for all types of ISEs shown in this thesis (potassium, hydrogen and chloride). 100 µL of ISM cocktail was diluted with 100 µL of THF. The GCE/PEDOT:PSS (or GCE/PEDOT:Cl^-) modified electrodes were placed face up in a plastic cup holder and 10 µL of diluted ISM cocktail was dropped and smeared over the surface of the electrode so that it covers both the ECP layer and the PVC surface around it. A needle was used to get rid of the bubbles formed while applying the ISM cocktail. The electrodes were left to dry until the following day, upon which they were immersed in the suitable conditioning solution (0.01 M KCl for potassium and chloride ISEs and 0.01 M HCl for hydrogen ISEs) for at least 24 hours before further measurements.

10. 6. Potentiometry experiments

Automatic calibrations were performed at room temperature (23±2°C) using 16-channel millivoltmeter (Lawson Labs. Inc., Malvern, PA, USA) and Metrohm Dosino 800 instrument equipped with two burettes of 50 mL volume (Herisau, Switzerland). 100.0 mL of 0.01 M KCl or HCl (in deionized water or in 0.1 M NaCl as background electrolyte) was pipetted into an electrochemical cell and respective ISEs, together with the reference electrode (double junction Ag/AgCl/3 M KCl/ 1 M LiOAc for potassium and chloride ISEs or single junction Ag/AgCl/3 M KCl for hydrogen ISEs), were placed inside the cell through a plastic holder. The Lawson potentiometer was set for measuring for 125 min. The automatic dilution system was first rinsed twice and 20 dilution steps were used – 38.2 mL of the solution in the electrochemical cell is sucked out and replaced with 38.2 mL of deionized water (or background electrolyte, 0.1 M NaCl). This accounts for a change of 0.21 units in the logarithm of activity of the primary ion ($\log a_i$). Each dilution took 5 minutes waiting time, to let the potential of the system stabilize. The potentials were collected every 5 seconds, and the last 5 points before the change in potential due to dilution were taken and averaged and this average value was used in further calculations. The slopes were usually calculated for the range of loga from -5 to -2. Activities were used instead of concentrations, calculated according to the extended Debye-Hückel equation.[84]

For addition/dilution potentiometric experiments, 50.0 mL of 1 mM KCl or HCl (in deionized water or background electrolyte, 0.1 M NaCl) was pipetted into the electrochemical cell, mounted on a magnetic stirrer and equipped with the respective ISE. The reference electrode used was a double junction Ag/AgCl/3 M KCl/ 1 M LiOAc for potassium and chloride ISEs or a single junction Ag/AgCl/3 M KCl for hydrogen ISEs. The electrodes were connected to a 16-channel millivoltmeter (Lawson Labs. Inc., Malvern, PA, USA). A sequential addition/dilution regime was adopted – 25.0 μL of 0.1 M KCl or HCl (in deionized water or background electrolyte, 0.1 M NaCl) was added, followed by 2.50 mL of deionized water or 0.1 M NaCl, followed by 26.5 μL of 0.1 M KCl or HCl (in deionized water or in 0.1 M NaCl as background electrolyte) and finally with 2.60 mL of deionized water or 0.1 M NaCl. This accounts for the change in concentration of 5%, back and forth, from 1 mM to 1.05 mM and from 1.05 mM to 1 mM KCl or HCl, respectively. After each addition/dilution step, a 5 minute waiting time was used to allow for the potential to stabilize.

For water-layer test experiment, the instrumental setup was the same as described previously. The purpose of performing this test was to check if there is a water layer formation between the solid contact and the ISM.[96] SCISEs were first conditioned in 0.1 M solution of either KCl (for potassium and chloride SCISEs) or 0.1 M HCl (for hydrogen SCISEs) for 24 hours after which their potential was measured for a few hours. The solution was then changed to 0.1 M NaCl (in the case of potassium and hydrogen SCISEs) or 0.1 M Na_2SO_4 (in the case of chloride SCISEs) and the potential was measured for a few hours. Then the solution was changed back to the original 0.1 M KCl (or HCl) and again the potential was measured for a few hours.

10. 7. Cyclic voltammetry experiments

The cyclic voltammetry experiments were performed for checking the polishing process of the electrodes and to check if the PEDOT:PSS (PEDOT:Cl^-) film formation on the surface of the electrode had been successful. The experiments were carried out using a three-electrode electrochemical cell connected to an Autolab General Purpose Electrochemical System (AUTO30.FRA2-Autolab Eco Chemie, B.V., The Netherlands). The working electrode was the previously mentioned GCE (area 0.071 cm^2) in the case of polishing check or GCE/ PEDOT:PSS (GCE/PEDOT:Cl^-) in the case of checking the film formation, the auxiliary electrode was a GC rod and the reference electrode Metrohm single junction Ag/AgCl/3 M KCl reference electrode. The experiments were performed in 0.1 M KCl, which was previously deaerated with N_2. The following parameters were used:

Table 3. CV parameters and their respective values

Starting potential	200 mV
Lowest potential	-500 mV
Highest potential	+500 mV
Scan rate	100 mV/s
Number of scans	2

10. 8. Chronoamperometry (coulometry) experiments

All chronoamperometry (coulometry) experiments were performed using a three-electrode electrochemical cell connected to an IviumCompactStat instrument (Ivium Technologies, The Netherlands). 50.0 mL of 1 mM KCl or HCl (in deionized water or in 0.1 M NaCl as background electrolyte) was pipetted into the electrochemical cell, mounted on a magnetic stirrer and equipped with the respective ISE, reference electrode (double junction Ag/AgCl/3 M KCl/ 1 M LiOAc for potassium and chloride ISEs or single junction Ag/AgCl/3 M KCl for hydrogen ISEs) and a GC rod as the counter electrode. A sequential addition-dilution regime was adopted – 25.0 μL of 0.1 M KCl or HCl (in deionized water or in 0.1 M NaCl as background electrolyte) was added, followed by 2.50 mL of deionized water or 0.1 M NaCl, followed by 26.5 μL of 0.1 M KCl or HCl (in deionized water or background electrolyte, 0.1 M NaCl) and finally with 2.60 mL of deionized water or 0.1 M NaCl. This accounts for the change in concentration of 5%, back and forth, from 1 mM to 1.05 mM and from 1.05 mM to 1 mM KCl or HCl, respectively. Before every coulometric experiment a chronopotentiometric measurement (using IviumCompactStat) was done for 10 minutes to check the potential of the ISE at hand in order to obtain the open circuit potential which will be set for the chronoamperometry experiment. The additions were performed when the current level reaches zero value with maximum ±1 nA drift.

10. 9. Electrochemical impedance spectroscopy experiments

EIS experiments were conducted for all of the prepared electrodes, using IviumCompactStat instrument (Ivium Technologies, The Netherlands). The conventional three-electrode electrochemical cell was used, equipped with the respective ISE, single junction Metrohm Ag/AgCl/3 M KCl reference electrode and GC rod counter electrode. The solutions were deaerated for 15 minutes by purging them with N_2 prior to EIS experiment. For potassium and chloride ISEs, 0.1 M KCl solution was used, while for the hydrogen ISEs, a commercial buffer solution (pH=7.00) was used instead. The following conditions were used:

Table 4. EIS parameters and their respective values

Conditioning potential	0 V
Amplitude potential	10 mV
Lowest frequency	10 mHz
Highest frequency	100 kHz
Number of frequencies	71

11. Results and discussion

For every type of electrode, be it SCISE or only ECP modified GCE, a triplicate of electrodes was prepared. Unless otherwise stated, the results are shown for one of the replicates, while other two replicates are shown in the **Appendix**.

11. 1. Potassium SCISEs

11. 1. 1. Potentiometric measurements

The calibration of the potassium SCISEs was performed in KCl solutions in the concentration range 10^{-2} to 10^{-6} M, either in deionized water or 0.1 M NaCl as background electrolyte (BE). The linear range was found to be 10^{-2} to 10^{-5} M (**Appendix A**), with the following calibration parameters (**Table 5**):

Most of the results have shown near-Nernstian slopes, which were in the range of the slopes earlier described for this method[11,12] and were thus deemed acceptable for further addition/dilution experiments using potentiometry and chronoamperometry methods.

Table 5. Potentiometry calibration data for potassium SCISEs

GCE/PEDOT:PSS/K^+ ISM					
Without background electrolyte			With background electrolyte (0.1 M NaCl)		
Electrode	Slope (mV)	Intercept (mV)	Electrode	Slope (mV)	Intercept (mV)
Replicate 1	59.1	191.2	Replicate 1	51.7	175.7
Replicate 2	59.0	277.3	Replicate 2	56.0	253.5
Replicate 3	59.6	176.1	Replicate 3	52.7	160.3
GCE/PEDOT:Cl^-/K^+ ISM					
Without background electrolyte			With background electrolyte (0.1 M NaCl)		
Electrode	Slope (mV)	Intercept (mV)	Electrode	Slope (mV)	Intercept (mV)
Replicate 1’	58.0	309.8	Replicate 1’	55.3	290.5
Replicate 2’	57.8	258.5	Replicate 2’	56.0	238.3
Replicate 3’	59.0	200.4	Replicate 3’	55.9	188.0

The results of addition/dilution experiments performed in the potentiometric transduction regime have shown that the presence of BE significantly influences the measurement (**Figures 13 and 14**). Having the BE increases the noise level so that the change in potential, caused by 5% changes in concentration, cannot be detected and measured. This provides a limitation to

the measurement, as the usual application for potassium ISEs is in clinical analysis, e.g. blood serum, where the concentration of sodium chloride is at the level of 0.14 M.[89,90] On the other hand, when no background electrolyte is used, a ca. 1.2 mV change can be measured, but it is superimposed on a constant drift of the potential. The observed potential drift can be caused by the low polymerization charge of the polymer film, 2 mC, since the PEDOT modified SCISEs usually show stable potential due to high redox capacitance of PEDOT.[45] Also, the drift could be due to the formation of the water-layer between the ISM and the ECP,[91] in which case a more hydrophobic ECP, like poly(3-octylthiophene) or poly(2-n-tetradecyl-2,3-dihydrothieno-[3,4-b][1,4]dioxine), should be sought for instead of PEDOT.[92,93] As will be shown later, the chronoamperometric measurements do not suffer from this limitation of BE (interfering ions), making their use advantageous compared to the classical potentiometric measurements with SCISEs.

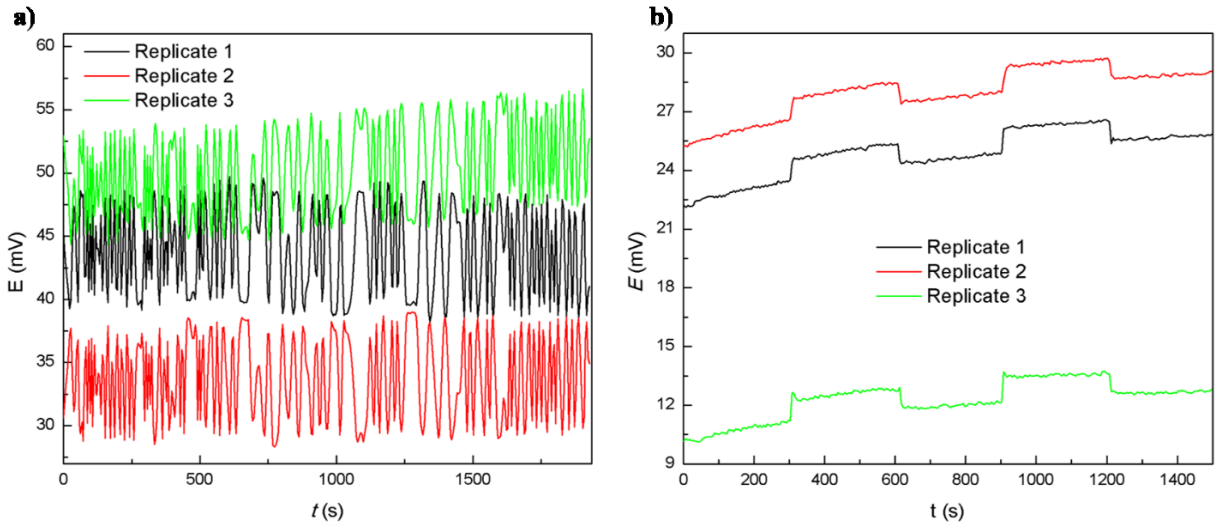

Figure 13. Potentiometric response of the potassium SCISEs (GCE/PEDOT:PSS/K^+ ISM) during the addition/dilution experiment with (a) and without (b) the background electrolyte. The changes in concentration, performed sequentially were of 5%, back and forth, from 1 mM to 1.05 mM and from 1.05 mM to 1 mM KCl, respectively.

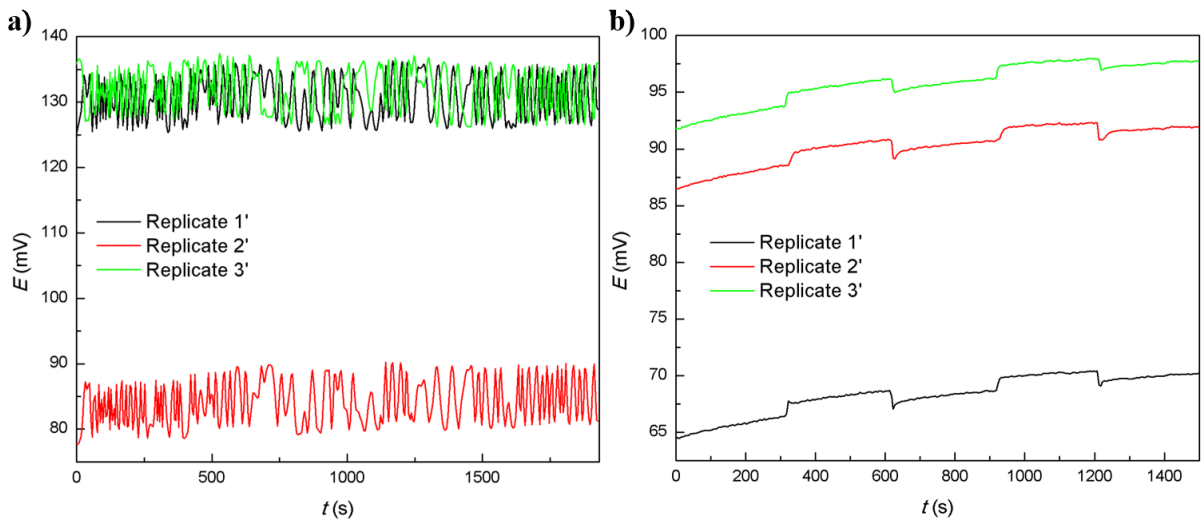

Figure 14. Potentiometric response of the potassium SCISEs (GCE/PEDOT:Cl^-/K^+ ISM) during the addition/dilution experiment with (a) and without (b) the background electrolyte. The changes in concentration, performed sequentially were of 5%, back and forth, from 1 mM to 1.05 mM and from 1.05 mM to 1 mM KCl, respectively.

11. 1. 2. Chronoamperometry (coulometry) experiments

Chronoamperometry (coulometry) results indicate that there is no apparent difference in using PEDOT:PSS or PEDOT:Cl^- as solid contacts in potassium SCISEs. Similarly to potentiometry, chronoamperometry measurements show that the results are superimposed on a drift, which is most probably due to the potential drift, as described before.[91] Interestingly, different from potentiometry results, chronoamperometry measurements seem to have higher drifts when the BE is not present than when it is (**Figures 15 and 16**). This may indicate that the supporting electrolyte plays a role in this new type of signal transduction method, most probably as the ohmic drop between the working and the counter electrodes, where the analyte ions partake in the passage of current through the solution. This interferes with the stability of the potential of the working electrode and, thus, leads to increased noise levels.[48,78,80] The average response (equilibration) time for both PEDOT:PSS and PEDOT:Cl^- based potassium SCISEs was determined as the time at which the current signal has decayed by 95% (equivalent to the time constant of the theoretical model of an RC circuit).[13] For GCE/PEDOT:PSS/K^+ ISM electrodes it was on average 67 s with and without BE present, while for GCE/PEDOT:Cl^-/K^+ ISM the equilibration times were 69 s and 67 s, with and without BE, respectively (**Table 6**). This signified that there was no considerable difference and thus no conclusive preference to be given to either of the two ECPs in this type of signal transduction. Compared to hydrogen and chloride SCISEs, for which the average equilibration time was in the order of several seconds (as it will be shown below), the equilibration time of the potassium SCISEs is several (ca. ten)

times higher. It is assumed that the ion transport through the membrane takes place in the form of ion-ionophore complex, which should not be exceedingly faster for hydrogen than the potassium ions.[94] In their previous work Han et al. have suggested that the rate and reversibility of PEDOT redox processes, as well as the rate and reversibility of the bulk and SCISE interfacial ion-transport processes should be kept in mind.[11] As later results with GCE/PEDOT:PSS and GCE/PEDOT:Cl^- electrodes will show, the average equilibration times for addition/dilution experiments performed in KCl solutions (for potassium responsive GCE/PEDOT:PSS) were on average 6 s, while in HCl solutions the equilibration times were less than a second, almost instantaneous. Bobacka et al. have previously indicated that the PEDOT films in aqueous solutions contain an excess of supporting electrolyte, facilitating ion diffusion and resulting in high values of diffusional pseudocapacitance.[63] Knowing that the diffusion constants of ions are related to their mobilities via the Einstein equation and since the mobility of hydrogen ions is ca. five times higher than that of the potassium or chloride ions,[95] the results would indicate that the diffusion is playing some role in the equilibration times of potassium, hydrogen and chloride SCISEs with PEDOT as solid contact.

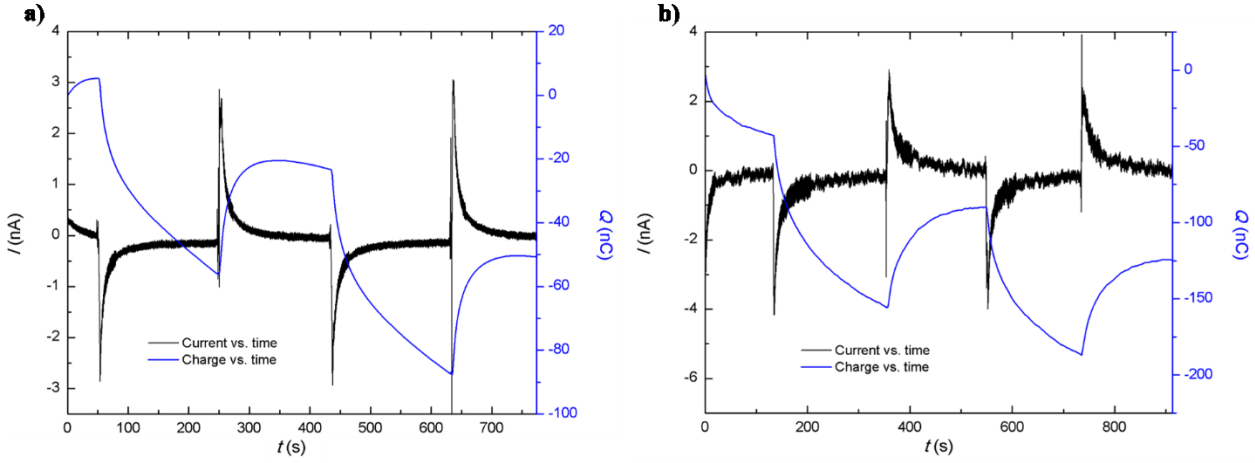

Figure 15. Chronoamperometry (coulometry) response of the potassium SCISEs (GCE/PEDOT:PSS/K^+ ISM) during the addition/dilution experiment with (a) and without (b) the BE, 0.1 M NaCl. The changes in concentration, performed sequentially were of 5%, back and forth, from 1 mM to 1.05 mM and from 1.05 mM to 1 mM KCl, respectively. The measurements were performed with the applied potential equal to the open-circuit potential measured prior to the experiment

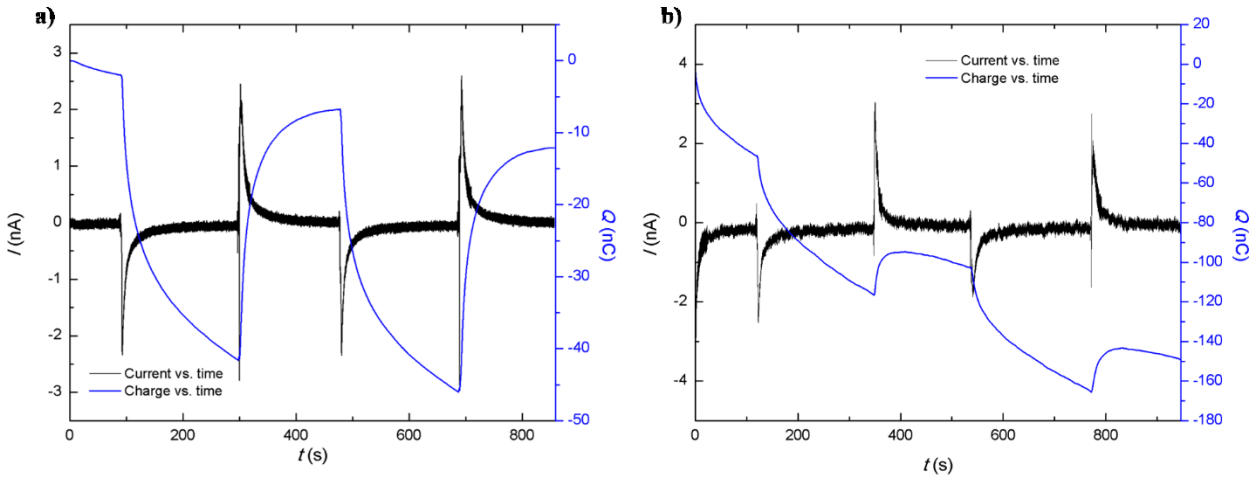

Figure 16. Chronoamperometry (coulometry) response of the potassium SCISEs (GCE/PEDOT:Cl^-/K^+ ISM) during the addition/dilution experiment with (a) and without (b) the BE, 0.1 M NaCl. The changes in concentration, performed sequentially were of 5%, back and forth, from 1 mM to 1.05 mM and from 1.05 mM to 1 mM KCl, respectively

Table 6. Equilibration times for potassium SCISEs

Electrode	Experimental setup	t_{av} (s)*	s_d (s)*
GCE/PEDOT:PSS/K^+ ISM	Without BE	67	9
	With BE (0.1 M NaCl)	67	9
GCE/PEDOT:Cl^-/K^+ ISM	Without BE	67	7
	With BE (0.1 M NaCl)	69	7

*n=12

11. 1. 3. Water-layer test

The water-layer test was performed as described by Lindner et al. by keeping the potassium SCISE for at least twenty four hours in 0.1 M KCl, then changing it to 0.1 M NaCl for three hours and finally bringing the SCISEs back to 0.1 M KCl for additional six hours.[96] As described by Lindner et al, the drift in the potential in KCl solution comes from the water-layer which is present between the PEDOT film and the ISM, while the drift of potential in NaCl solution comes from the perturbance of the membrane composition due to the ion exchange of sodium ion from the solution and potassium ions from the membrane. If the water layer formation occurs, the exchange of sodium ions will create a "reservoir" of interfering ions in the water layer, leading to a permanent drift of potential, as seen after returning the ISE back into KCl solution.[96] The results shown in **Figure 17** indicate that the water-layer formation was not critical for these electrodes, even though in the **Appendix D** some electrodes are shown to have potential drifts, which would be expected for electrodes with PEDOT films and not significantly hydrophobic membranes.[91,96] Be that as it may, these results do indicate that a further improvement should be made in potential stability of thin-layer drop cast SCISEs by using more hydrophobic ISMs and ECPs.

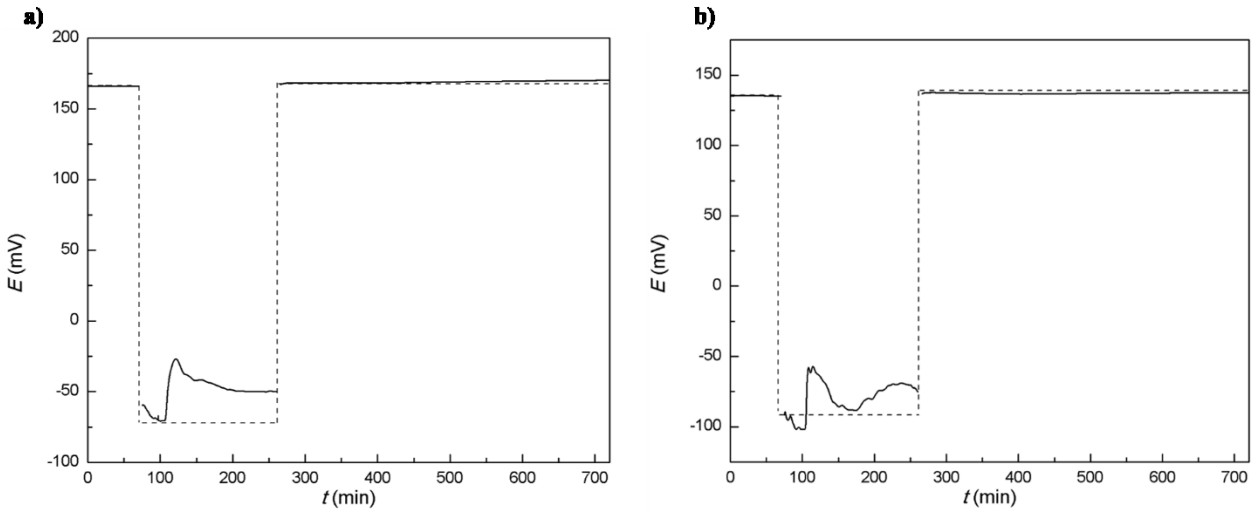

Figure 17. Potentiometric response of the potassium SCISEs (GCE/PEDOT:PSS/K^+ ISM, replicate 1, a, and GCE/PEDOT:Cl^-/ K^+ ISM, replicate 1', b) during the water-layer test in which the electrodes were first immersed in 0.1 M KCl solution, followed by immersion into 0.1 M NaCl and finally into 0.1 M KCl solution again

11. 1. 4. Electrochemical impedance spectroscopy

The EIS experiments were performed in order to probe the mechanism of electrochemical processes occurring in the bulk solution and at the potassium SCISEs interface. The electrochemical impedance spectra were collected in the frequency range of 100 kHz to 10 mHz (**Figure 18**). The high frequency range of the Nyquist plot shown in **Figure 18** indicates the presence of the ISM with resistance corresponding to the diameter of the semicircle. The resistances, shown in the **Appendix E** are 5 and 10 times higher than those of hydrogen SCISEs and potassium SCISEs, respectively. However, the lower frequency part shows a tail of impedances with an angle of ca. 48° for potassium SCISEs with PEDOT:PSS as solid contact and ca. 51° for potassium SCISEs with PEDOT:Cl^- as solid contact, quite close to 45°. This means that the Warburg impedance, due to diffusion of potassium ions to and from the SCISE, plays a role in the performance of these electrodes, but it is not yet certain whether this is the limiting factor for the equilibration time. These results agree with the results previously obtained by Han et al.[11] The difference in impedances at lower frequencies for GCE/PEDOT:PSS/K^+ ISM (**Figure 18a**) electrodes is in agreement with the variability in their slope, most probably due to the difference in the formed PEDOT:PSS solid contact.

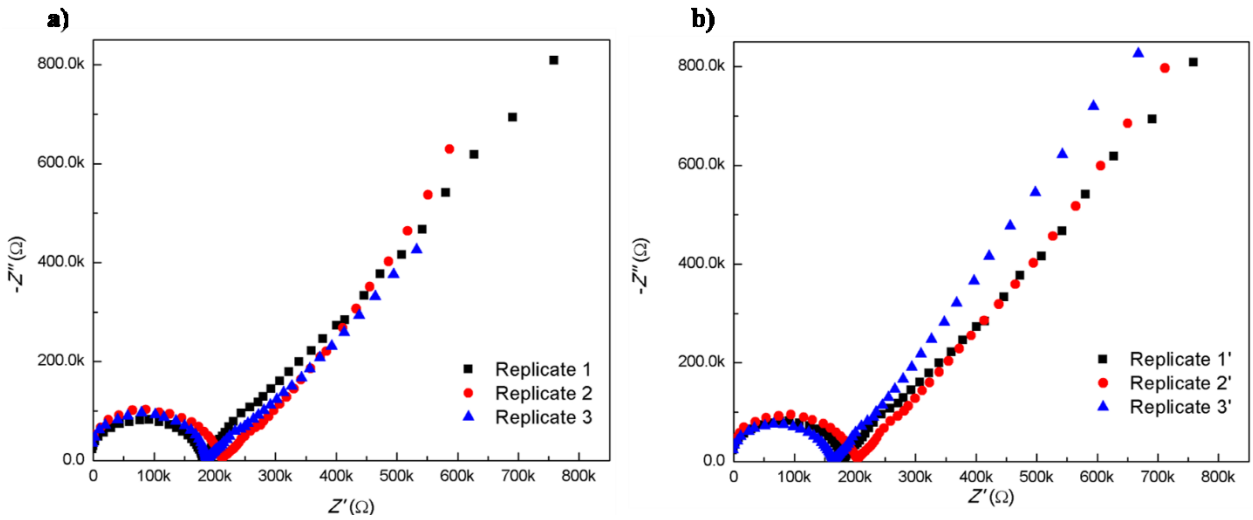

Figure 18. Electrochemical impedance spectra of potassium SCISEs – a) GCE/PEDOT:PSS/K^+ ISM and b) GCE/PEDOT:Cl^-/ K^+ ISM, recorded in 0.1 M KCl solution with the excitation potential of 10 mV and in the frequency range of 100 kHz to 10 mHz

11. 2. Hydrogen SCISEs

11. 2. 1. Potentiometry experiments

The calibration of the hydrogen SCISEs was performed in HCl solutions, together with a pH glass electrode, in the concentration range 10^{-2} to 10^{-6} M, either in deionized water or in 0.1 M NaCl as background electrolyte (BE). The linear range was found to be 10^{-2} to 10^{-5} M (**Appendix A**) only for the GCE/PEDOT:Cl^-/H^+ ISM SCISEs, with the following calibration parameters (**Table 7**):

Table 7. Potentiometry calibration data for hydrogen SCISEs

GCE/PEDOT:PSS/H^+ ISM					
Without background electrolyte			With background electrolyte (0.1 M NaCl)		
Electrode	Slope (mV)	Intercept (mV)	Electrode	Slope (mV)	Intercept (mV)
Replicate 1	-38.3	224.9	Replicate 1	-46.8	335.9
Replicate 2	-31.6	170.2	Replicate 2	-38.0	266.1
Replicate 3	-24.1	224.0	Replicate 3	-41.4	302.0
GCE/PEDOT:Cl^-/H^+ ISM					
Without background electrolyte			With background electrolyte (0.1 M NaCl)		
Electrode	Slope (mV)	Intercept (mV)	Electrode	Slope (mV)	Intercept (mV)
Replicate 1’	-47.8	389.8	Replicate 1’	-15.6	285.4
Replicate 2’	-54.4	418.9	Replicate 2’	-44.6	354.4
Replicate 3’	-53.5	407.5	Replicate 3’	-21.9	287.7
Glass El.	-54.6	635.2	Glass El.	-57.0	657.6

The obtained results were acceptable for further measurements in addition/dilution experiments with potentiometry and chronoamperometry only in the case of GCE/PEDOT:Cl^-/H^+ ISM SCISEs, as they were shown to have slopes which were comparable to the glass electrode.

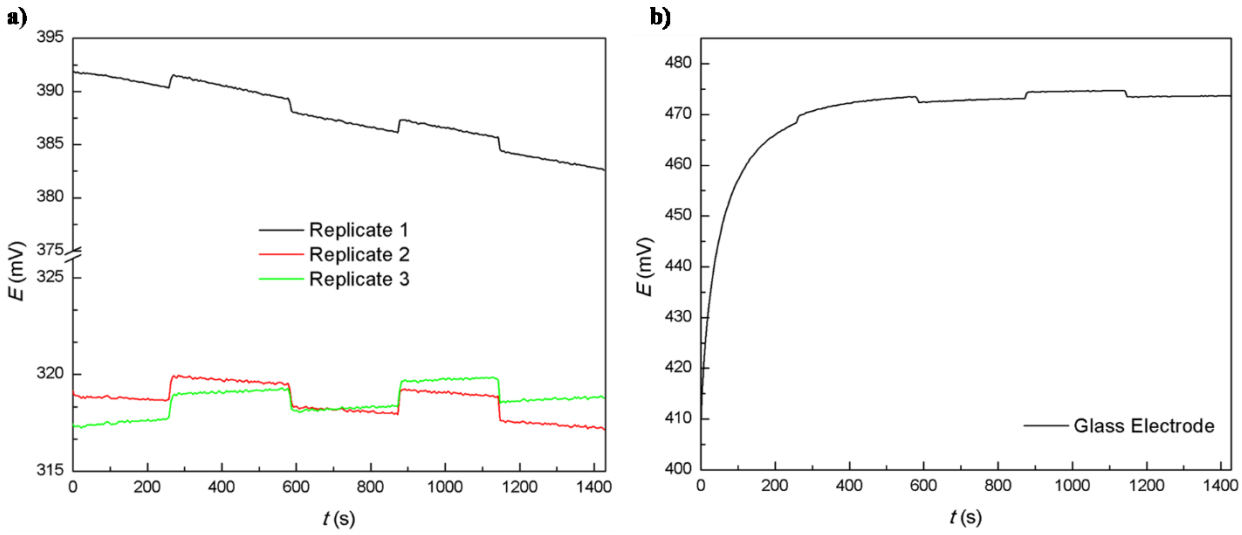

Figure 19. Potentiometric response of the hydrogen SCISE (GCE/PEDOT:Cl^-/H^+ ISM a), and pH glass electrode b) during the addition/dilution experiment. The changes in concentration, performed sequentially were of 5%, back and forth, from 1 mM to 1.05 mM and from 1.05 mM to 1 mM HCl, respectively

The addition/dilution experiment has shown that the electrodes change their potential similar to the pH glass electrode (**Figure 19**). Still, unable to be calibrated in the presence of the background electrolyte, these electrodes probably suffer from the water-layer and interfering ion "reservoir" formation between the ISM and the solid contact, and the introduction of more hydrophobic solid contact and/or ISM would increase the electrodes' potential stability.

11. 2. 2. Chronoamperometry (coulometry) experiments

The results obtained without the background electrolyte show an extremely fast response of the hydrogen SCISEs (**Figure 20**), yet with higher level of noise compared to potassium and chloride SCISEs (**Figures 15 and 24**). The equilibration times, which were on average 8 s (s_d=2, n=12) are comparable to the equilibration times of chloride SCISEs (**Figure 24**) and are ca. ten times lower in comparison with potassium SCISEs. Since the resistances of GCE/PEDOT:Cl-/H^+ ISM and chloride SCISEs are ca. 20 kΩ (**Figures 22 and 26**), which is ten times lower than the resistances of potassium SCISEs (**Figure 18**), these results may indicate a possible correlation between equilibration times and ISM resistances. On the other hand, hydrogen SCISEs show higher current noise compared to potassium and chloride SCISEs (with no BE), which was also observed with GCE/PEDOT:PSS and GCE/PEDOT:Cl^- electrodes in HCl solutions (**Figures 27 and 29**). The reason for this remains unknown,

although it indicates that the measurements involving hydrogen ions are influenced more by the presence of the background solution compared to others.

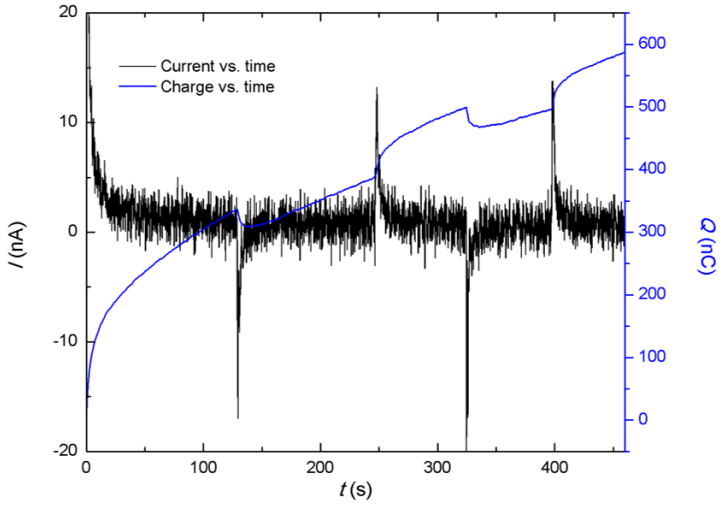

Figure 20. Chronoamperometry (coulometry) response of the hydrogen SCISE (GCE/PEDOT:Cl^-/H^+ ISM) during the addition/dilution experiment without the BE. The changes in concentration, performed sequentially were of 5%, back and forth, from 1 mM to 1.05 mM and from 1.05 mM to 1 mM HCl, respectively

11. 2. 3. Water-layer test

As described with potassium SCISEs, the water-layer test was performed as described by Lindner et al. by keeping the hydrogen SCISE for at least twenty four hours in 0.1 M HCl, then changing it to 0.1 M NaCl for three hours and finally bringing the SCISEs back to 0.1 M HCl for additional six hours.[96] When exposed to the solution containing interfering ions, the potential of hydrogen SCISEs gets significantly perturbed (**Figure 21 and Appendix D**). Even if the potential of some electrodes were to return to its starting value, the results clearly show that the influence of water-layer formation is detrimental in these thin-layer ISM SCISEs and may be one of the reasons for their poor potentiometric behaviour.

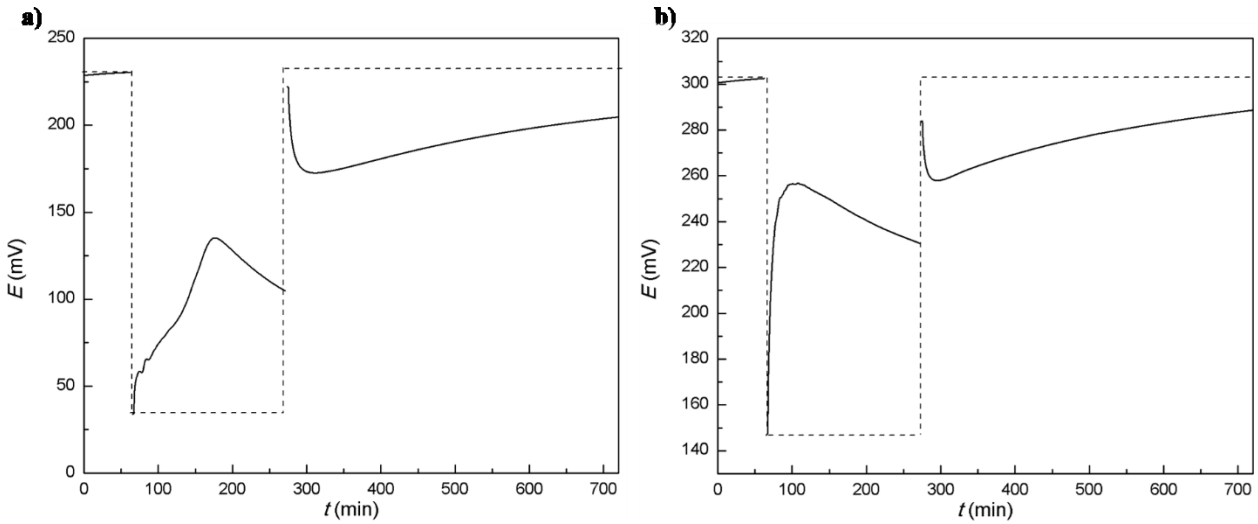

Figure 21. Potentiometric response for the hydrogen SCISEs (GCE/PEDOT:PSS/H^+ ISM, replicate 1 a) and GCE/PEDOT:Cl^-/ H^+ ISM, replicate 1' b) during the water-layer test in which the electrodes were first immersed in 0.1 M HCl solution, followed by immersion into 0.1 M NaCl and finally into 0.1 M HCl solution again

11. 2. 4. Electrochemical impedance spectroscopy

The EIS experiments were performed in order to probe the mechanism of electrochemical processes occurring in the bulk solution and at the hydrogen SCISEs interface. The electrochemical impedance spectra were collected in the frequency range of 100 kHz to 10 mHz (**Figure 22**), as for the other SCISEs, but in the commercial buffer solution of pH 7.00 rather than in 0.1 M KCl. Again, the high-frequency semicircle shown in **Figure 22** indicates the formation of the ISM with resistance corresponding to the diameter of the semicircle. The resistances (**Appendix E**) are ca. ten times lower than those for potassium SCISEs. However, the lower frequency part shows a tail of impedances with an angle of ca. 61° (PEDOT:PSS as solid contact) and ca. 64° (PEDOT:Cl^- as solid contact), meaning the Warburg impedance, probably coupled to a capacitive element, may play a role in the performance of these electrodes, similarly to potassium SCISEs. The slightly lower resistance value of Replicate 3' (**Figure 22b**) is concordant with it poorer potentiometric slope and indicates a poor membrane formation for this electrode. Even though the impedance spectra for GCE/PEDOT:PSS/H^+ ISM electrodes are very similar, their potentiometric response was shown to be very variable and worse compared to GCE/PEDOT:Cl-/H^+ ISM electrodes. One reason may be that the hydrogen electrodes show better responses in buffered solutions, where the effect of CO_2 from the air cannot influence the measurement.

Interestingly, these results differ from those reported by Han et al. for hydrogen SCISEs in 0.1 M HCl[70]. In their work, the lower frequency region is resembling that of an ideal capacitor with the incomplete semicircle, suggesting that diffusion does not play a key role in the transduction. One of the reasons for this discrepancy in results may by that different media for recording the spectrum are used. In the case of the buffer solution, the concentration of hydrogen ions is a million times lower than that of 0.1 M HCl, which may cause the diffusion limitation observed in the spectra.

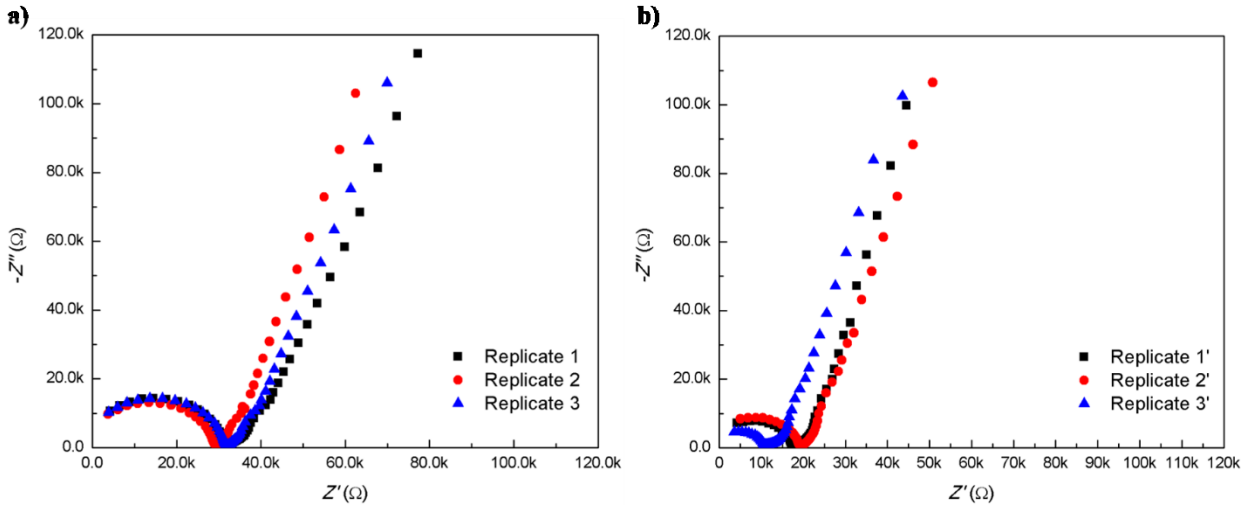

Figure 22. Electrochemical impedance spectra of hydrogen SCISEs (GCE/PEDOT:PSS/H^+ ISM a) and GCE/PEDOT:Cl^-/ H^+ ISM b), recorded in commercial buffer solution (pH=7.00) with the excitation potential of 10 mV and in the frequency range of 100 kHz to 10 mHz

11. 3. Chloride SCISEs

11. 3. 1. Potentiometry experiments

The calibration of chloride SCISEs was performed in KCl solutions in the concentration range 10^{-2} to 10^{-6} M. The linear range was found to be from 10^{-2} to 10^{-4} M (**Appendix A**). The obtained results are shown in **Table 8**:

Table 8. Potentiometry calibration data for chloride SCISEs

Electrode	Slope (mV)	Intercept (mV)
Replicate 1	-58.6	83.1
Replicate 2	-58.5	87.3
Replicate 3	-59.2	93.0

The slopes of chloride SCISEs were Nernstian and, thus, in agreement with the slopes earlier described for this method[11,12] and were thus deemed acceptable for further addition/dilution experiments with potentiometry and chronoamperometry.

The addition/dilution experiment, performed in the potentiometric mode as described before, shows that the electrode in potentiometric transduction regime will change its potential ca. 1.2 mV (**Figure 23**).

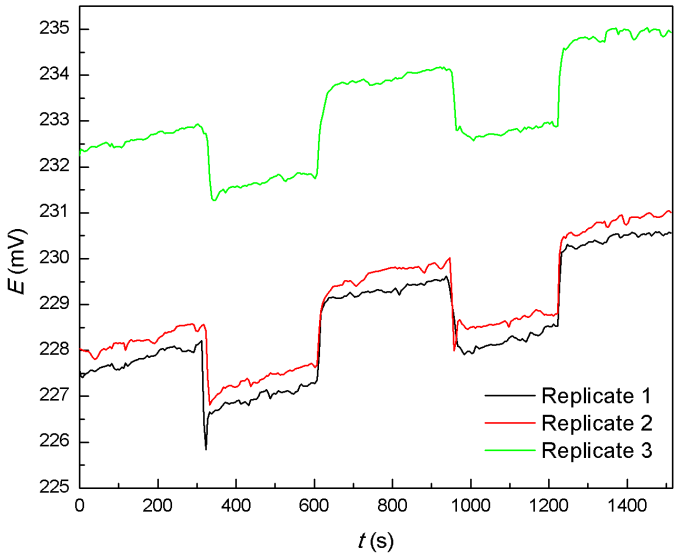

Figure 23. Potentiometric response of the chloride SCISEs (GCE/PEDOT:Cl^-/Cl^- ISM) during the addition/dilution experiment. The changes in concentration, performed sequentially were of 5%, back and forth, from 1 mM to 1.05 mM and from 1.05 mM to 1 mM KCl, respectively

As in all the previous cases of SCISEs, there was a constant potential drift during the potentiometry measurements, which was discussed in detail for potassium SCISEs in chapter 11. 1. 1.

11. 3. 2. Chronoamperometry (coulometry) experiments

The results obtained in chronamperometry measurements (**Figure 24 and Appendix B**) show that the equilibration times are different from that of potassium SCISEs, while they are much similar to the ones from hydrogen SCISEs. The equilibration times were on average 6 s (s_d=1 s, n=12), which is comparable to hydrogen SCISEs (average of 8 s with standard deviation of 2 s), but much lower when compared to potassium SCISEs, where the equilibration time was on average 67 s. Since the ion mobilities, and thus diffusion constants, of potassium and chloride ions in the bulk solution are comparable,[95] these results indicate that the diffusion in the bulk solution does not limit the novel transduction method in terms of equilibration times. It rather points in the direction of the ISM and the solid contact.

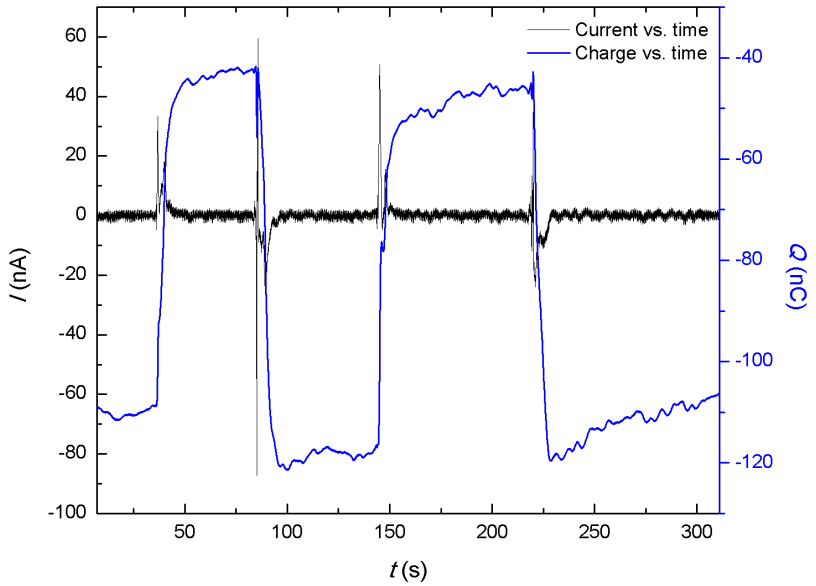

Figure 24. Chronoamperometric and chronocoulometry response of the chloride SCISEs (GCE/PEDOT:Cl^-/Cl^- ISM, replicate 1) during the addition/dilution experiment. The changes in concentration, performed sequentially were of 5%, back and forth, from 1 mM to 1.05 mM and from 1.05 mM to 1 mM KCl, respectively

11. 3. 3. Water-layer test

As with all other SCISEs, the water-layer test was performed by keeping the chloride SCISE for at least twenty four hours in 0.1 M KCl, then changing it to 0.1 M K_2SO_4 for three hours and finally bringing the SCISEs back to 0.1 M KCl for additional six hours.[96] When exposed to the solution containing interfering sulfate ions, the potential of chloride SCISEs gets significantly perturbed (**Figure 25 and Appendix D**). Not only does the potential drift significantly during the exposure to the solution of interfering ions, but even after the return to the original solution containing primary ions, the potential drift is considerably high. This may limit the expansion of application of these electrodes to real samples and should be considered if any further research into this area should take place.

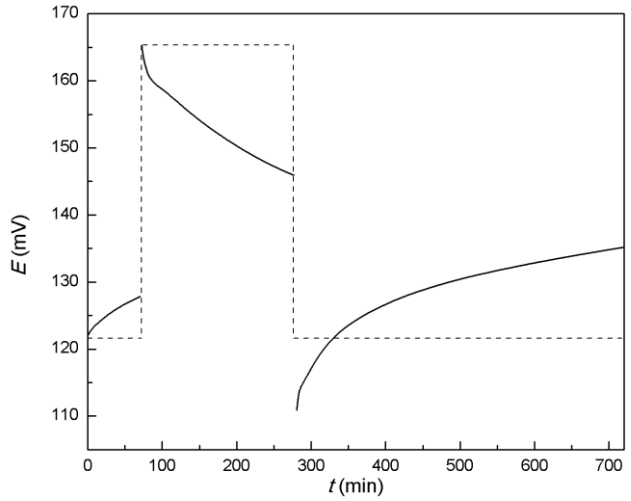

Figure 25. Potentiometric response of the chloride SCISEs (GCE/PEDOT:Cl^-/Cl^- ISM, replicate 1) during the water-layer test

11. 3. 4. Electrochemical impedance spectroscopy

The EIS measurements were performed in order to probe the mechanism of electrochemical processes occurring in the bulk solution and at the chloride SCISEs interface. The electrochemical impedance spectra were collected in the frequency range of 100 kHz to 10 mHz (**Figure 26**). The high frequency range of the Nyquist plot shown in **Figure 26** indicates the formation of the ISM with resistance corresponding to the diameter of the semicircle. The resistances of chloride SCISEs (**Table 9 and Appendix E**) are lower than those for potassium SCISEs and are comparable to those of hydrogen SCISEs (**Figures 18 and 22**). However, the lower frequency part shows a tail of impedances with an angle of ca. 84°, which approaches that of an ideal capacitor (90°). This means that the Warburg impedance, due to diffusion of chloride ions to and from the SCISE, does not play a critical role in the performance of these electrodes, as the chronoamperometric results have suggested. Knowing that the ion mobility of chloride is almost five times lower than the ion mobility of protons in the aqueous solution,[95] and that the diffusion does not influence the chloride SCISEs, it is obvious that the chloride ISM, with the ion-exchanger salt, has a much faster rate of ion transport through the membrane compared with ionophore based ISMs. This further indicates that the equilibration times are influenced by the rate of the ion transport through the membrane, so the mobilities of ions or ion-ionophore complexes should be considered in the construction of SCISEs, so as to obtain the optimal analytical parameters in the coulometric signal transduction method.[97-99]

In their earlier work, Jarolímová et al. have proposed a theoretical model for the coulometric signal transduction method, based on a simple RC circuit which they have tested on chloride SCISEs.[13] According to the proposed model, the equilibration time is dependent on the resistance of the membrane, R_{cell} and the capacitance of the ECP, C_{cp}. Since the capacitance is proportionally related to the polymerization charge of the ECP film, kept constant for all of the prepared electrodes, the only influencing factor to the difference in equilibration times of potassium, hydrogen and chloride SCISEs would come from the resistance of the ISM, R_{cell}. The comparison of SCISE resistances and equilibration times seem to be correlated (**Table 9**).

Table 9. Resistances of potassium, hydrogen and chloride SCISEs shown as average of measurements with three SCISEs

Electrode	$R_{cell,\ average}$*	t_{av} (s)**	s_d (s)**
GCE/PEDOT:PSS/K^+ ISM	197	69	7
GCE/PEDOT:Cl^-/K^+ ISM	186	67	7
GCE/PEDOT:Cl^-/H^+ ISM	18	8	2
GCE/PEDOT:Cl^-/Cl^- ISM	18	6	1

*n=3

**n=12

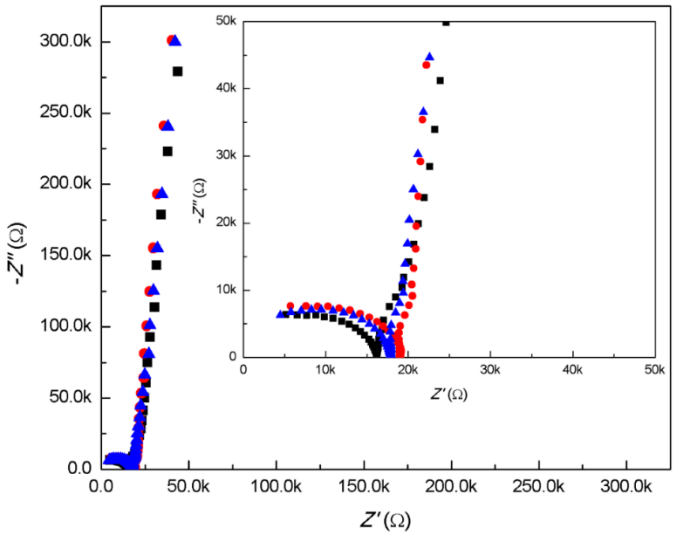

Figure 26. Electrochemical impedance spectra of three chloride SCISEs, recorded in 0.1 M KCl solution with the excitation potential of 10 mV and in the frequency range of 100 kHz to 10 mHz with zoomed high frequency region (inset)

11. 4. GCE/PEDOT:PSS electrodes

11. 4. 1.Cyclic voltammetry

CV results (**Appendix F**) show that the formation of PEDOT:PSS layer was successful and that it exhibits a usual capacitor-like shape, close to rectangular.[63] The deviation from the ideal rectangular shape can also be due to the low polymerization charge of the polymer film (2 mC).

11. 4. 2. Potentiometry experiments

The calibration of the GCE/PEDOT:PSS modified electrodes was performed in KCl and HCl solutions in the concentration range 10^{-2} to 10^{-6} M, both in deionized water. The GCE/PEDOT:PSS electrodes were conditioned in 0.01 M KCl (or HCl) at least 24 hours before performing the calibration. The linear range was found to be from 10^{-2} to 10^{-5} M (**Appendix A**), with the following calibration parameters (**Table 10**):

Table 10. Potentiometry calibration data for GCE/PEDOT:PSS electrodes

Calibration in KCl			Calibration in HCl		
Electrode	Slope (mV)	Intercept (mV)	Electrode	Slope (mV)	Intercept (mV)
Replicate 1	46.7	215.9	Replicate 1’	53.9	374.3
Replicate 2	44.5	203.3	Replicate 2’	54.2	372.4
Replicate 3	44.6	201.3	Replicate 3’	54.3	375.8

Interestingly, GCE/PEDOT:PSS electrodes show slopes in the HCl calibration which are comparable to the hydrogen SCISEs and the pH glass electrode! Of course, it should be kept in mind that GCE/PEDOT:PSS electrodes do not exhibit selectivity to hydrogen over other ions, compared with hydrogen SCISEs and pH glass electrode.

11. 4. 3. Chronoamperometry (coulometry) experiments

The chronoamperometry (coulometry) results for GCE/PEDOT:PSS modified electrodes show significant difference between addition/dilution experiments performed in KCl and HCl solutions (**Figure 27 and Appendix B**). The equilibration time for GCE/PEDOT:PSS in KCl solution is on average 6 s (s_d=1 s, n=12), while in the HCl solution it is less than a second, almost instantaneous. This correlates well with the assumption that for bare PEDOT films the mobilities of ions in the bulk solution significantly influence the signal transduction. When performed in HCl, the chronoamperometric measurements have shown several times higher noise levels in comparison with the measurements performed in KCl solutions. This is quite similar to the behaviour of hydrogen SCISEs which show pronounced current noise compared to potassium and chloride SCISEs. The reason for this noise level increase remains unclear.

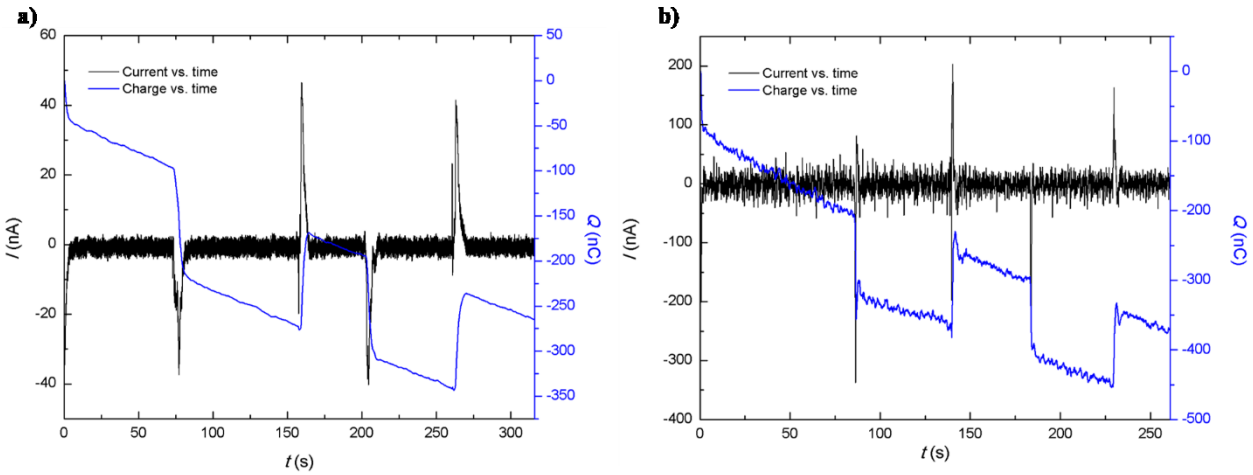

Figure 27. Chronoamperometric and chronocoulometry response of the GCE/PEDOT:PSS (replicate 1) modified electrode during the addition/dilution experiment in KCl solution (a) and HCl solution (b). The changes in concentration, performed sequentially, were of 5%, back and forth, from 1 mM to 1.05 mM and from 1.05 mM to 1 mM KCl (HCl), respectively

11. 4. 5. Electrochemical impedance spectroscopy

The impedance spectra of PEDOT:PSS films were recorded in 0.1 M KCl and the commercial buffer solution of pH=7.00. The impedance spectra of PEDOT:PSS resemble those of an ideal capacitor, with a slight deviation from ideality most probably due to the parallel faradaic reaction occurring between oxygen and PEDOT:PSS film.[100] This type of PEDOT films was previously studied by Bobacka et al. who have stated that the semblance of capacitor behaviour indicates the involvement of all redox sites of the polymer in the doping process.[45,63] When the spectra are recorded in the buffer solution (**Figure 28b**), points at lower frequencies tend to slightly bend, most probably due to the combined effect of oxygen presence and the faradaic pseudocapacitance of PEDOT. Since the content of the commercial buffer is unknown, some faradaic processes occurring due to the presence of certain unidentified ions cannot be excluded.

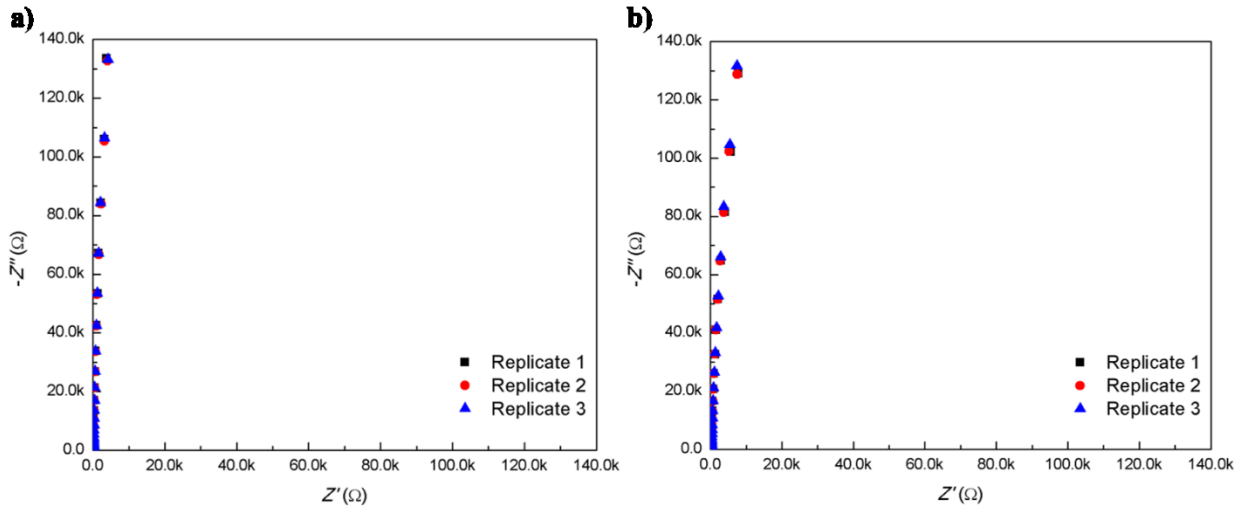

Figure 28. Electrochemical impedance spectra of GCE/PEDOT:PSS modified electrodes, recorded in 0.1 M KCl (a) and in commercial buffer solution of pH=7.00 (b) with the excitation potential of 10 mV and in the frequency range of 100 kHz to 10 mHz

11. 5. GCE/PEDOT:Cl⁻ electrodes

11. 5. 1. Cyclic voltammetry

CV results (**Appendix F**) show that the formation of PEDOT:Cl^- layer was successful and that it exhibits a usual capacitor-like shape, close to rectangular.[63] The deviation from the ideal rectangular shape can also be due to the low polymerization charge of the polymer film (2 mC).

11. 5. 2. Potentiometry experiments

The calibration of the GCE/PEDOT:Cl^- modified electrodes was performed in KCl and HCl solutions in the concentration range 10^{-2} to 10^{-6} M, both in deionized water. The GCE/PEDOT:Cl^- electrodes were conditioned in 0.01 M KCl (or HCl) at least 24 hours before performing the calibration. The linear range was found to be from 10^{-2} to 10^{-5} M (**Appendix A**), with the following calibration parameters (**Table 11**):

Table 11. Potentiometry calibration data for GCE/PEDOT:Cl^- electrodes

Calibration in KCl			Calibration in HCl		
Electrode	Slope (mV)	Intercept (mV)	Electrode	Slope (mV)	Intercept (mV)
Replicate 1	-24.4	103.7	Replicate 1’	-13.2	263.9
Replicate 2	-51.8	75.9	Replicate 2’	-47.7	176.1
Replicate 3	-52.1	72.7	Replicate 3’	-47.9	173.9

Only one replicate was dismissed in both cases due to the low sensitivity, most probably due to problems with electrode’s surface.

11. 5. 3. Chronoamperometry (coulometry) experiments

The chronoamperometry (coulometry) results for GCE/PEDOT:Cl^- modified electrodes (**Figure 29**) show significant difference compared to the results obtained GCE/PEDOT:PSS modified electrodes (**Figure 27**). Compared to the results obtained with GCE/PEDOT:PSS in KCl solution (**Figure 27**a), the PEDOT:Cl^- modified electrodes show several times lower equilibration times, on average 1 s (s_d=1 s, n=12). Knowing that the potassium and chloride ion mobilities in the bulk solution are of comparable magnitude,[95] the results are a clear indication of different ionic transductions in PEDOT:PSS and PEDOT:Cl^- polymer films. The results obtained in HCl solutions (**Figure 27b**) show comparable noise levels to the ones recorded with PEDOT:PSS in HCl solution. But, even though two different ion transductions take place, cationic in case of PEDOT:PSS and anionic in case of PEDOT:Cl^-, the equilibration times are comparably instantaneous. This proves that the ionic rate of transduction through the polymer film differs depending on the doping ion, even for bulk ions of comparable ion mobility.

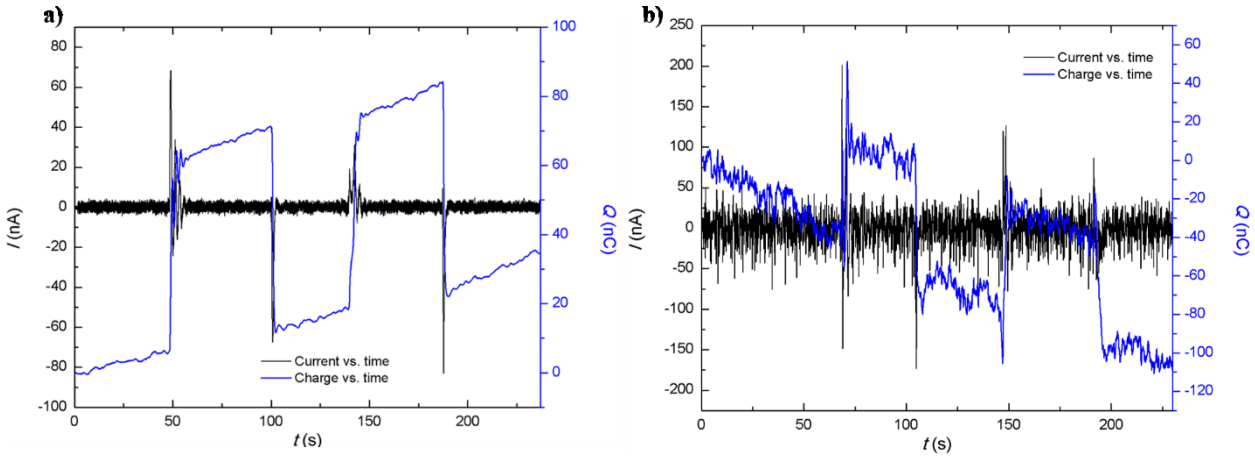

Figure 29. Chronoamperometric and chronocoulometry response of the GCE/PEDOT:Cl^- modified electrode (replicate 1) during the addition/dilution experiment in KCl solution (a), and in HCl solution (b). The changes in concentration, performed sequentially, were of 5%, back and forth, from 1 mM to 1.05 mM and from 1.05 mM to 1 mM KCl (or HCl), respectively

11. 5. 4. Electrochemical impedance spectroscopy

The impedance spectra of PEDOT:Cl^- films were recorded either in 0.1 M KCl or in the commercial buffer solution of pH=7.00. The impedance spectra of PEDOT: Cl^- resemble those of an ideal capacitor, with a slight deviation from ideality most probably due to the parallel faradaic reaction occurring between oxygen and PEDOT:Cl^- film,[100] as was previously discussed for PEDOT:PSS and it is another example of how all redox sites of the polymer are

involved in the doping process.[45, 63] When the spectra are recorded in the buffer solution (**Figure 30b**), points at lower frequencies tend to bend more prominently than in the case of PEDOT:PSS. In this case, the faradaic reactions occurring between the polymer and certain unspecified ions present in the buffer solution may be the shifting the Nyquist plot towards diffusion limited Warburg impedance at lower frequencies.

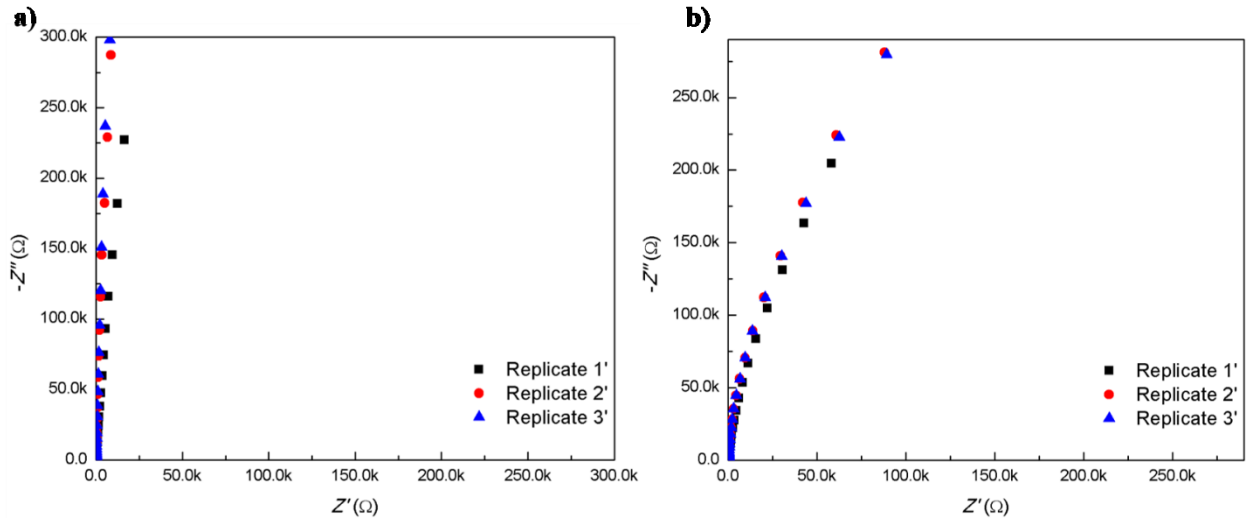

Figure 30. Electrochemical impedance spectra of GCE/PEDOT:Cl^- modified electrodes, recorded in 0.1 M KCl (a), and in commercial buffer solution of pH=7.00 (b) with the excitation potential of 10 mV and in the frequency range of 100 kHz to 10 mHz

12. Conclusions

The novel coulometric signal transduction method was studied by comparing potentiometry and chronoamperometry (coulometry) techniques. Three types of thin-layer SCISEs were prepared – potassium, hydrogen and chloride, using a modified drop-casting procedure. Furthermore, PEDOT:PSS and PEDOT:Cl^- modified GCEs, without ISMs, were tested similarly.

When tested in the addition/dilution experiments, with potentiometric signal transduction, the potassium SCISEs have shown to be prone to noise in the presence of high concentration of interfering sodium ions and the small changes in concentration of potassium ions at low concentration potassium solution cannot be detected and measured. On the other hand, when no interfering ions are present, the hydrogen and chloride SCISEs can be used to measure small changes in concentration even at millimolar level. However, the inability to calibrate most of the hydrogen SCISEs in these conditions have implied the need for a different hydrogen SCISE preparation. Additionally, all electrodes were prone to potential drifts. When the same addition/dilution experiments were performed with coulometric signal transduction, this type

of interfering ion limitation was not observed for either of the SCISEs. What is more, the presence of interfering ions, in the form of background electrolyte (BE), proved to be beneficial in terms of reducing the current noise in chronoamperometric measurements.

Water-layer tests performed for potassium, hydrogen and chloride SCISEs have shown that hydrogen and chloride SCISEs are more prone to water-layer formation compared to potassium SCISEs. Taking this into account, further preparation of SCISEs for coulometric signal transduction should also focus on the composition of the ISM, increasing its hydrophobicity, e.g. by adding salts with both hydrophobic ions, like ETH 500 in the case of potassium ISM.

Interestingly, chronoamperometric (coulometric) measurements have shown differences in equilibration times of potassium SCISEs compared to hydrogen and chloride SCISEs, which were comparable. The equilibration times of potassium SCISEs we ca. ten times higher than those of hydrogen and chloride SCISEs, which seems to be in correlation with ISM resistance and additionally backs the theoretical RC circuit model presented for chloride SCISEs. Besides the equilibration times, differences were observed when using BE. With no BE present, the noise in chronoamperograms of potassium SCISEs increases, most probably due to the ohmic drop and the participation of primary ions in the passage of current through the bulk solution, which disturbs the potential stability of the working electrode. Electrochemical impedance spectra have shown that Warburg impedance, due to diffusion of ions to and from the electrode, is present primarily in potassium SCISEs, while low frequency EIS region of hydrogen and chloride SCISEs shows more capacitor-like behaviour. This type of behaviour is implicative of the fact that the membrane resistance and rate of transport through the membrane play the major role in signal transduction, with diffusion starting to play a role only at sufficiently high ISM resistances.

The chronoamperograms of PEDOT:PSS modified GCEs show difference in cases of potassium and hydrogen ion transduction, with equilibration times for potassium being several times higher than for hydrogen, showing that ion-to-electron transduction is diffusion limited in the case of PEDOT:PSS polymer films. On the contrary, PEDOT:Cl^- modified GCEs show comparably quick, rather instantaneous, response towards chloride. Given that the ion mobility of potassium and chloride ions in the bulk solution are of the same scale, these results have indicated different ion transduction rate in the PEDOT:Cl^- polymer film compared with PEDOT:PSS.

13. References

1. Cattrall W. R, *Chemical Sensors*, 1st ed, 1997, Oxford University Press Inc, Great Clarendon Street, Oxford OX2 6DP, Great Britain

2. Harwood E. J. The use of an ion-selective electrode for routine fluoride analyses on water samples. *Water Research*, **1969**, *3*, 273-280.

3. Clarke L. W.; Cox D.; Gonder-Frederick A. L.; Carter W.; Pohl L. S. Evaluating Clinical Accuracy of Systems for Self-Monitoring of Blood Glucose. *Diabetes Care*, **1987**, *10*, 622-628.

4. Forster J. R; Keyes E. T. Ion-selective Electrodes in Environmental Analysis. In *Encyclopedia of Analytical Chemistry*, 1st ed.; John Wiley & Sons, Ltd. 2006; pp 1-21.

5. Amman D.; Malinowska E.; Oech U.; Schefer U.; Simon W. Ion Selective Electrodes (ISE's) in Clinical Chemistry. In *Clinical Chemistry: An Overview*, 1st ed.; den Boer N. C.; van der Heiden C.; Leijnse B.; Souverijn J. H. M. Plenum Press: New York, 1989, pp. 269-276.

6. Bobacka J. Conducting Polymer-Based Solid-State Ion-Selective Electrodes. *Electroanalysis*, **2006**, *18*, 7-18.

7. Bandodkar J. A.; Jeerapan I.; Wang J.; Wearable Chemical Sensors: Present Challenges and Future Prospects. *ACS Sensors*, **2016**, *1*, 464-482.

8. Wolfbeis S. O. Probes, Sensors and Labels: Why is the Real Progress Slow? *Angewandte Chemie International Edition*, **2013**, *52*, 9864-9865.

9. Hupa E.; Vanamo U.; Bobacka J. Novel Ion-To-Electron Principle for Solid-Contact ISEs. *Electroanalysis*, **2015**, *27*, 591-594.

10. Han T.; Vanamo U.; Bobacka J. Influence of Electrode Geometry on the Response of Solid-Contact Ion-Selective Electrodes when Utilizing a New Coulometric Readout Method. *ChemElectroChem*, **2016**, *3*, 2071-2077.

11. Bobacka J.; Han T.; Mattinen U. Improving the Sensitivity of Solid-Contact Ion-Selective Electrodes by Using Coulometric Signal Transduction. *Analytical Chemistry*, **2019**, *4*, 900-906.

12. Vanamo U.; Hupa E.; Vanamo U.; Yrjänä V.; Bobacka J. New Signal Readout Principle for Solid-Contact Ion-Selective Electrodes, *Analytical Chemistry*, **2016**, *88*, 4369-4374.

13. Jarolimova Z.; Han T.; Mattinen U.; Bobacka J.; Bakker E. Mattinen U. Capacitive Model for Coulometric Readout of Ion-Selective Electrodes. *Analytical Chemistry*, **2018**, *90*, 8700-8707.

14. Hulanicki A.; Glab S.; Ingman F. Chemical Sensors Definitions and Classification. *Pure and Applied Chemistry*, **1991**, *63*, 1247-1250.

15. J. Janata, *Principles of Chemical Sensors*, 2nd ed, 2010, Springer Science+Business Media, 233 Spring Street, New York, NY 10013, USA

16. Eggins R. B, *Chemical Sensors and Biosensors*, 1st ed, 2002, John Wiley & Sons, Ltd, Baffins Lane, Chichester, West Sussex, PO19 1UD, England

17. Belyustin A. A. The centenary of glass electrode: from Max Cremer to F. G. K. Baucke. *Journal of Solid State Electrochemistry*, **2011**, *15*, 47-65.

18. Cremer M.; Haupt K. Ober die Ursache der elektromotorischen Eigenschaften derGewebe, Zugleich ein Beitrag zur Lehre von den polyphasischen Elektrolytketten. *Zeitschrift fur Biologie*, **1906**, *47*, 562-2504.

19. Bakker E.; Telting-Diaz M. Electrochemical Sensors. *Analytical Chemistry*, **2002**, *74,* 2781-2800.

20. Janata J.; Josowicz M. DeVaney D. M.; Chemical Sensors. *Analytical Chemistry*, **1994**, *66,* 207R-228R.

21. Janata J. Chemical Sensors. *Analytical Chemistry*, **1992**, *64,* 196R-219R.

22. Moore C.; Pressman C.B. Mechanism of Action of Valinomycin on Mitochondria. *Biochemical and Biophysical Research Communications*, **1964**, *15,* 562-567.

23. Radu A.; Radu T.; McGraw C.; Dillingham P.; Anastasova-Ivanova S.; Diamond D. Ion selective electrodes in environmental analysis. *Journal of the Serbian Chemical Society*, **2013**, *78,* 1729-1761.

24. Shirakawa H. The discovery of polyacetylene film – The dawning of an era of conducting polymers. *Synthetic Metals*, **2002**, *125,* 3-10.

25. Taniguchi I.; Fujiyasu T.; Tomimura S.; Eguchi H.; Yasukouchi K.; Tsuji I.; Unoki M. A Potentiometric Immunoglobulin G Sensor Based on a Polypyrrole Modified Platinum Electrode. *Analytical Sciences*, **1986**, *2,* 587-588.

26. Ikariyama Y.; Heineman R. W. Polypyrrole Electrode as a Detector for Electroinactive Anions by Flow Injection Analysis. *Analytical Chemistry*, **1986**, *58,* 1803-1806.

27. Thackeray W. J.; Wrighton S. M. Chemically Responsive Microelectrochemical Devices Based on Platinized Poly(3-methylthiophene): Variation in Conductivity with Variation in Hydrogen, Oxygen or pH in Aqueous Solution. *Journal of Physical Chemistry*, **1986**, *90,* 6674-6679.

28. Cadogan A.; Gao Z.; Lewenstam A.; Ivaska A.; Diamond D. All-solid-state sodium-selective electrode based on a calixarene ionophore in a poly(vinyl chloride) membrane with a polypyrrole solid contact. *Analytical Chemistry*, **1992**, *64*, 2496-2501.

29. Pretsch E. The new wave of ion-selective electrodes. *Trends in Analytical Chemistry*, **2007**, *26*, 46-51.

30. Bakker E.; Pretsch E. The New Wave of Ion-Selective Electrodes. *Analytical Chemistry*, **2002**, *74*, 420A-426A.

31. Fucsko J.; Toth K.; Pungor E.; Kunovits J.; Puxbaum H. Application of ion-selective electrodes in environmental analysis: Determination of Acid and Fluoride concentrations in Rain-water with a Flow-Injection System. *Analytica Chimica Acta*, **1987**, *194*, 163-170.

32. Durst A. R.; Scheide P. E. Indirect Determination of Sulfate in Natural Waters by Ion-Selective Electrode. *Analytical Letters*, **1977**, *10*, 55-65.

33. De Marco R.; Clarke G.; Pejcic B. Ion-Selective Electrode Potentiometry in Environmental Analysis. *Electroanalysis*, **2007**, *19*, 1987-2001.

34. Yu R. T. Application of Ion-Selective Electrodes in Soil Science. *Ion-Selective Electrode Reviews*, **1985**, *7*, 165-202.

35. Arvand M.; Asadollahzadeh S. A. Ion-selective electrode for aluminum determination in pharmaceutical substances, tea leaves and water samples. *Talanta*, **2008**, *75*, 1046-1054.

36. Hulstein J. J. J.; van ‘t Sant P. Sweat analysis using indirect ion-selective electrode on the routine chemistry analyser meets UK guidelines. *Annals of Clinical Biochemistry*, **2011**, *48*, 374-376.

37. D’Orazio P. Biosensors in clinical chemistry. *Clinica Chimica Acta*, **2003**, *334*, 41-69.

38. Aglan F. R.; Saleh M. H. ; Mohamed G. G.; Potentiometric determination of mercury (II) ion in various real samples using novel modified screen-printed electrode. *Applied Water Science*, **2018**, *8*, 141-151.

39. Bakker E.; Pretsch E. Potentiometric sensors for trace-level analysis. *Trends in Analytical Chemistry*, **2005**, *24*, 199-207.

40. Dimeski G.; Badrick T.; St John A. Ion Selective Electrodes (ISEs) and interferences – A review. *Clinica Chimica Acta*, **2010**, *411*, 309-317.

41. Levy G. B. Determination of Sodium With Ion-Selective Electrodes. *Clinical Chemistry*, **1981**, *27*, 1435-1438.

42. Athavale R.; Kokorite I.; Dinkel C.; Bakker E.; Wehril B.; Crespo A.; G. Brand A. In Situ Ammonium Profiling Using Solid-Contact Ion-Selective Electrodes in Eutrophic Lakes. *Analytical Chemistry*, **2015**, *87*, 11990-11997.

43. Michalska A. All -Solid-State Ion Selective and All-Solid-State Reference Electrodes. *Electroanalysis*, **2012**, *24*, 1253-1265.

44. Hu J.; Stein A.; Bühlman P. Rational design of all-solid-state ion-selective electrodes and reference electrodes. *Trends in Analytical Chemistry*, **2016**, *76*, 102-114.

45. Bobacka J. Potential Stability of All-Solid-State Ion-Selective Electrodes Using Conducting Polymers as Ion-to-Electron Transducers. *Analytical Chemistry*, **1999**, *71*, 4932-4937.

46. Mikhelson N. K. Ion-selective electrodes in PVC matrix. *Sensors and Actuators B: Chemical*, **1994**, *18*, 31-37.

47. Imoto M.; Sakaki T.; Osakai T. Sophisticated Design of PVC Membrane Ion-Selective Electrodes Based on the Mixed Potential Theory. *Analytical Chemistry*, **2013**, *85*, 4753-4760.

48. Wang J, *Analytical Electrochemistry*, 2nd ed, 2000, A John Wiley & Sons, Inc. 605 Third Avenue, New York, NY 10158-0012, USA

49. Craggs M.; Moody J. G.; Thomas D. R. J. PVC matrix membrane ion-selective electrodes. Construction and laboratory experiments. *Journal of Chemical Education*, **1974**, *51*, 541-544.

50. Beer P. D. Molecular and ionic recognition by chemical methods. In *Chemical Sensors*, 1st ed.; Edmonds T. E. Chapman and Hall: New York, 1988; pp 17-69.

51. Armstrong D. R.; Horvai G. Properties of PVC based membranes used in ion-selective electrodes. *Electrochimica Acta*, **1990**, *35*, 1-7.

52. Bakker E.; Pretsch E. Lipophilicity of tetraphenylborate derivatives as anionic sites in neutral carrier-based solvent polymeric membranes and lifetime of corresponding ion-selective electrochemical and optical sensors. *Analytica Chimica Acta*, **1995**, *309*, 7-17.

53. Amman D.; Pretsch E.; Simon W.; Lindner E.; Bezegh A.; Pungor E. Lipophilic salts as membrane additives and their influence on the properties of macro- and micro-electrodes based on neutral carriers. *Analytica Chimica Acta*, **1985**, *171*, 119-129.

54. Mikhelson N. K. *Ion-Selective Electrodes*, 2nd ed, 2010, Springer Verlag, Tiergartenstrase 17, Berlin, Heidelberg, Germany

55. Buhlmann P.; Chen D. L. Ion-Selective Electrodes With Ionophore-Doped Sensing Membranes. In *Supramolecular Chemistry: From Molecules to Nanomaterials*, 1st ed.; Steed W. J.; John Wiley & Sons, Ltd: New York, 2012; pp 2539-2580.

56. Feast W. J. Conducting polymers. In *Chemical Sensors*, 1st ed.; Edmonds T. E. Chapman and Hall: New York, 1988; pp 117-130.

57. De Survile R.; Jozefowicz M.; Yu T.; Perichon J.; Buvet R. Electrochemical Chains Using Protolytic Organic Semiconductors. *Electrochimica Acta*, **1968**, *13*, 1451-1458.

58. Wise D. D *Electrical and Optical Polymer Systems: Fundamentals, Methods and Applications* , 1st ed, 1998, Marcel Dekker, Inc. 270 Madison Avenue, New York, New York 10016, USA

59. Gvozdenović M. M.; Jugović Z. B.; Stevanović S. J.; Grgur B. Electrochemical Synthesis of Electroconducting Polymers. *Hemijska industrija*, **2014**, *68*, 673-684.

60. Inzelt G. *Conducting Polymers – A New Era in Electrochemistry*, 1st ed, 2008, Springer Verlag, Tiergartenstrase 17, Berlin, Heidelberg, Germany

61. Boeva A. Zh.; Sergeyev G. V. Polyaniline: Synthesis, Properties and Application. *Polymer Science, Series C*, **2014**, *56*, 144-153.

62. Birch B. J; Edmonds T. E. Potentiometric transducers. In *Chemical Sensors*, 1st ed.; Edmonds T. E. Chapman and Hall: New York, 1988; pp 214-224.

63. Bobacka J.; Lewenstam A.; Ivaska A. Electrochemical impedance spectroscopy of oxidized poly(3,4-ethylenedioxythiophene) film electrodes in aqueous solutions. *Journal of Electroanalytical Chemistry*, **2000**, *489*, 17-27.

64. Satoh N.; Otsuka M.; Ohki T.; Ohi A.; Sakurai Y.; Yamashita Y.; Mori T. Organic π-type thermoelectric module supported by photolithographic mold: A working hypothesis of sticky thermoelectric materials. *Science and Technology of Advanced Materials*, **2018**, *19*, 517–525.

65. Vázquez M.; Bobacka J.; Ivaska A.; Lewenstam A. Influence of oxygen and carbon dioxide on the electrochemical stability of poly(3,4-ethylenedioxythiophene) used as ion-to-electron transducer in all-solid-state ion-selective electrodes. *Sensors and Actuators B*, **2002**, *82*, 7-13.

66. Bobacka J.; Ivaska A.; Lewenstam A. Potentiometric Ion Sensors. *Chemical Reviews*, **2008**, *108*, 329-351.

67. Weber W. A.; O' Neil D. G.; Kounaves P. S. Solid Contact Ion Selective Electrodes for In Situ Measurements at High Pressure. *Analytical Chemistry*, **2017**, *89*, 4803-4807.

68. Nikolskii B. P.; Materova E. A. Solid Contact in Membrane Ion-Selective Electrodes. *Ion-Selective Electrode Reviews*, **1985**, *7*, 3-39.

69. Lewenstam A. Direct Solid Contact in Reference Electrodes. In *Handbook of Reference Electrodes*, 1st ed.; Inzelt G.; Lewenstam A.; Scholz F. Springer Verlag, Tiergartenstrase 17, Berlin, Heidelberg, Germany, 2013; pp 279-289.

70. Guth U.; Gerlach F.; Decker M.; Oelbner W.; Vonau W. Solid-state reference electrodes for potentiometric sensors. *Journal of Solid State Electrochemistry*, **2009**, *13*, 27-39.

71. Hauser C. P.; Wright A. G.; Chiang W. L. D. A potassium ion-selective electrode with valinomycin based poly(vinyl chloride) membrane and a poly(vinyl ferrocene) solid contact. *Analytica Chimica Acta*, **1995**, *302*, 241-248.

72. Lewenstam A. Routines and Challenges in Clinical Application of Electrochemical Ion-Sensors. *Electroanalysis*, **2014**, *26*, 1171-1181.

73. Cattrall W. R.; Freiser H. Coated Wire Ion Selective Electrodes. *Analytical Chemistry*, **1971**, *43*, 1905-1906.

74. Buck P. R. Ion Selective Electrodes. *Analytical Chemistry*, **1976**, *48*, 23R-39R.

75. Bobacka J.; Ivaska A.; Lewenstam A. Potentiometric Ion Sensors Based on Conducting Polymers. *Electroanalysis*, **2003**, *15*, 366-374.

76. Bakker E.; Bühlman P.; Pretsch E. Carrier-Based Ion-Selective Electrodes and Bulk Optodes. 1. General Characteristics. *Chemical Reviews*, **1997**, *97*, 3083-3132.

77. Bühlman P.; Pretsch E.; Bakker E. Carrier-Based Ion-Selective Electrodes and Bulk Optodes. 2. Ionophores for Potentiometric and Optical Sensors. *Chemical Reviews*, **1998**, *98*, 1593-1688.

78. A. Bard, L. R. Faulkner. *Electrochemical Methods – Fundamentals and Applications*, 2nd ed, 2000, A John Wiley & Sons, Inc. 605 Third Avenue, New York, NY 10158-0012, USA

79. D. A. Skoog, J.J. Leary, Principles of Instrumental Analysis, 4th ed, 1992, Saunders College Publishing, United States of America.

80. D. C. Harris, Quantitative Chemical Analysis, 8th ed, 2010 and 9th ed, 2015, W. H. Freeman and Company, New York, NY, United States of America.

81. Bakker E. Ion Selective Electrodes – Overview. In *Encyclopedia of Analytical Science: Reference Module in Chemistry, Molecular Sciences and Chemical Engineering*, 3rd ed.; Miró M.; Poole C.; Townshend A.; Worsfold P. Elsevier, 2019, pp. 231-251.

82. Ren K. Selectivity problems of membrane ion-selective electrodes – A method alternative to the IUPAC recommendation and its application to the selectivity mechanism investigation. *Fresenius Journal of Analytical Chemistry*, **1999**, *365*, 389-397.

83. Southampton Electrochemistry Group, University of Southampton, *Instrumental methods in electrochemistry*, 1st ed, 1990, Ellis Horwood, Woodhead Publishing, 1518 Walnut Street, Suite 1100, Philadelphia, PA 19102-3406, USA

84. Dvorak J.; Kavan L; Koryta J, *Principles of Electrochemistry*, 2nd ed, 1993, John Wiley & Sons, Ltd, Baffins Lane, Chichester, West Sussex, PO19 1UD, England

85. Koopal G. C.; Eijsma B.; Nolte J. M. R. Chronoamperometric detection of glucose by a third generation biosensor constructed from conducting microtubules of polypyrrole. *Synthetic Metals*, **1993**, *57*, 3689-3695.

86. Roberts Jr. L. J.; Sawyer T. D.; Sobkowiak A. *Electrochemistry for Chemists*, 2nd ed, 1995, John Wiley & Sons, Ltd, Baffins Lane, Chichester, West Sussex, PO19 1UD, England 79.

87. Myland C. J.; Oldham B. K. *Fundamentals of Electrochemical Science*, 1st ed, 1994, Academic Press, Inc, 1250 Sixth Avenue, San Diego, California 92101-4311, USA.

88. Macdonald R. J. Impedance Spectroscopy. *Annals of Biomedical Engineering*, **1992**, *20*, 289-305.

89. Lewenstam A.; Maj-Zurawska M.; Maj-Zurawska M. Application of Ion-Selective Electrodes in Clinical Analysis. *Electroanalysis*, **1991**, *3*, 727-734.

90. Shea M. A.; Hammill G. B.; Curtis H. L.; Szczech A. L.; Schulman A. K. Medical Costs of Abnormal Serum Sodium Levels. *Journal of the American Society of Nephrology*, **2008**, *19*, 764-770.

91. Fibbioli M.; Morf E. W.; Badertscher M.; de Rooij F. N. ; Pretsch E. Potential Drifts of Solid-Contacted Ion-Selective Electrodes Due to Zero-Current Ion Fluxes Through the Sensors Membrane. *Electroanalysis*, **2000**, *12*, 1286-1292.

92. Athavale R.; Dinkel C.; Wehrli B.; Bakker E.; Crespo A. G.; Brand A. Robust-Solid Contact Ion Selective Electrodes for High Resolution In Situ Measurements in Fresh Water Systems. *Environmental Science and Technology Letters*, **2017**, *4*, 286-291.

93. Guzinski M.; Jarvis M. J.; D'Orazio P.; Izadyar A.; Pendley D. B.; Lindner E. Solid-Contact pH Sensor without CO2 Interference with a Superhydrophobic PEDOT-C14 as Solid Contact: The Ultimate "Water Layer" Test. *Analytical Chemistry*, **2017**, *89*, 8468-8475.

94. Lindner E.; Zwickl T.; Bakker E.; Lan B. T. T.; Toth K.; Pretsch E. Spectroscopic *in situ* imaging of acid coextraction processes in solvent polymeric ion-selective electrode and optode membranes. *Analytical Chemistry*, **1998**, *70*, 1176−1181.

95. P. Atkins, J. de Paula, *Atkins' Physical Chemistry*, 8th ed, 2006, Oxford University Press Inc, Great Clarendon Street, Oxford OX2 6DP, Great Britain

96. Lindner E.; Gyurcsányi E. R. Quality control criteria for solid-contact, solvent polymeric membrane ion-selective electrodes. *Journal of Solid State Electrochemistry*, **2009**, *13*, 51-68.

97. Armstrong D. R.; Nikitas P. Transport of K^+ in PVC matrix membranes containing valinomycin. *Electrochimica Acta*, **1985**, *30*, 1627-1629.

98. Armstrong D. R.; Covington K. A.; Evans P. G. Relative mobilites of ions ion-selective electrodes with poly(vinyl chloride) membranes. *Analytica Chimica Acta*, **1985**, *166*, 103-109.

99. Armstrong D. R.; Todd M. Ionic mobilities in PVC membranes. *Electrochimica Acta*, **1987**, *32*, 155-157.

100. Vorotyntsev A. M.; Deslouis C.; Musiani M. M.; Tribollet B.; Aoki K. Transport across an electroactive polymer film in contact with media allowing both ionic and electronic interfacial exchange. *Electrochimica Acta*, **1999**, *44*, 2105-2115.

14. Appendices

Appendix A.

Potentiometric calibration curves for potassium hydrogen and chloride SCISEs, together with GCE/PEDOT:PSS and GCE/PEDOT:Cl^- electrodes, performed using sequential autodilution

GCE/PEDOT:PSS/K^+ ISM (without BE)

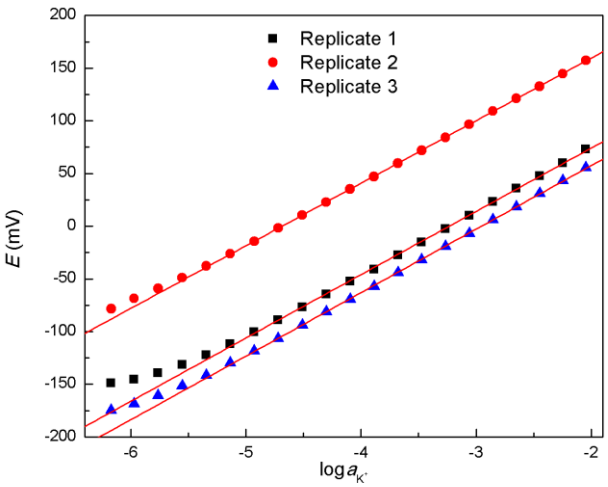

GCE/PEDOT:PSS/K^+ ISM (0.1 M NaCl BE)

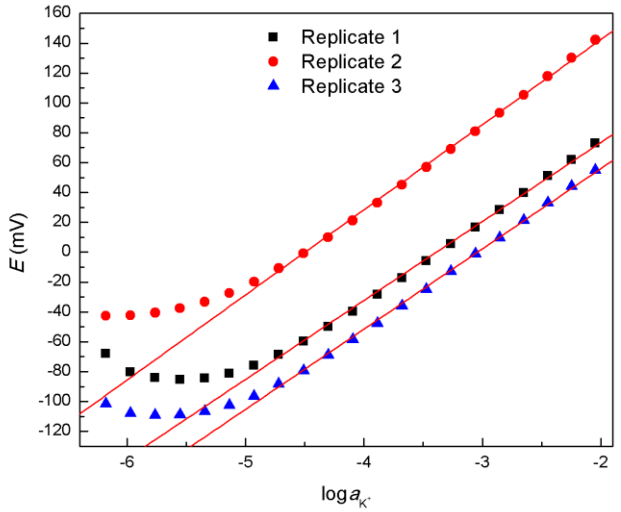

GCE/PEDOT:Cl^-/K^+ ISM (without BE)

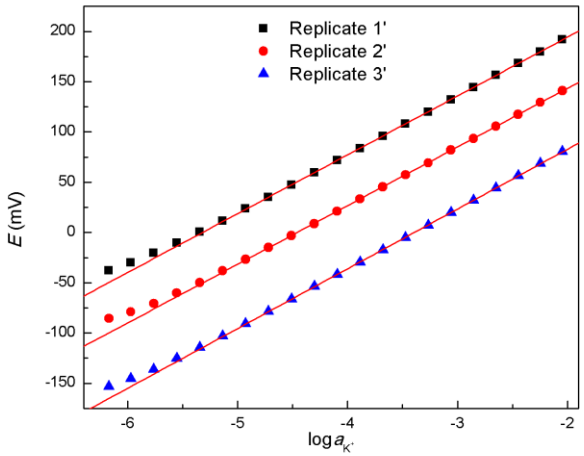

GCE/PEDOT:Cl^-/K^+ ISM (0.1 M NaCl BE)

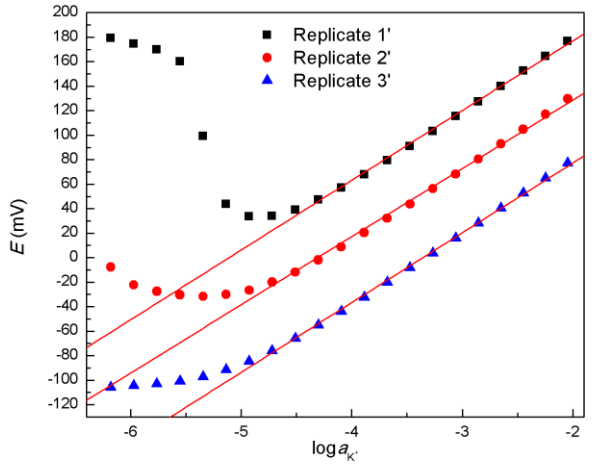

GCE/PEDOT:PSS/H^+ ISM (without BE)

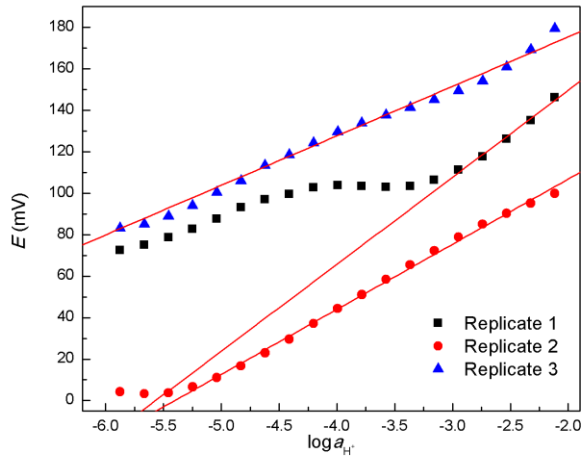

GCE/PEDOT:PSS/H^+ ISM (0.1 M NaCl BE)

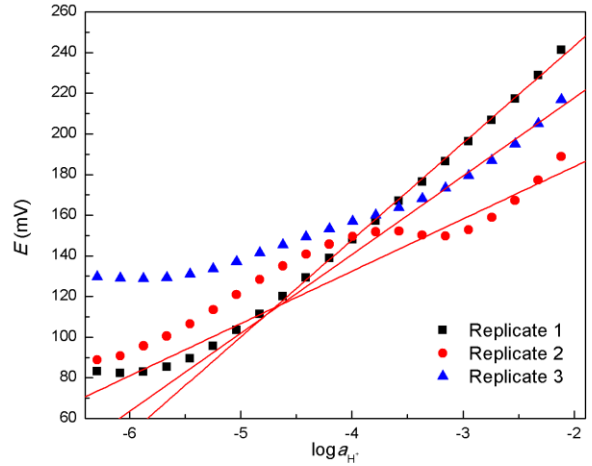

GCE/PEDOT:Cl^-/H^+ ISM (without BE)

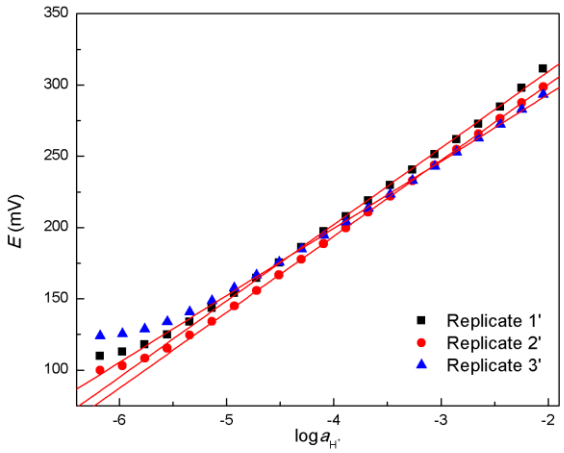

GCE/PEDOT:Cl^-/H^+ ISM (0.1 M NaCl BE)

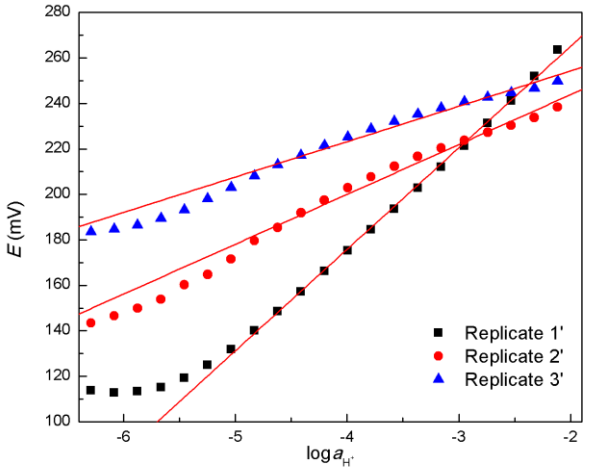

Glass electrode (without BE)

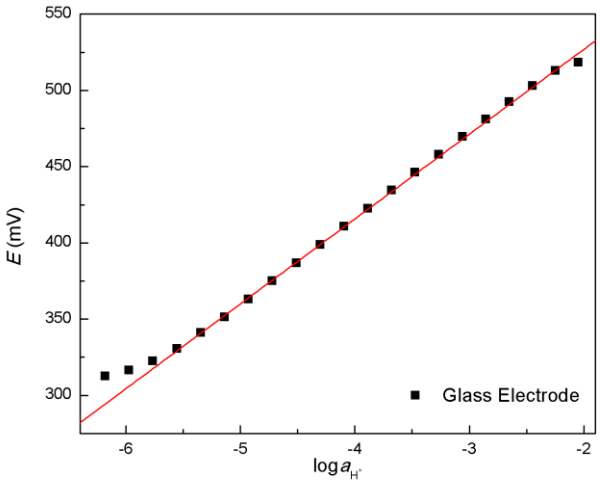

Glass electrode (0.1 M NaCl BE)

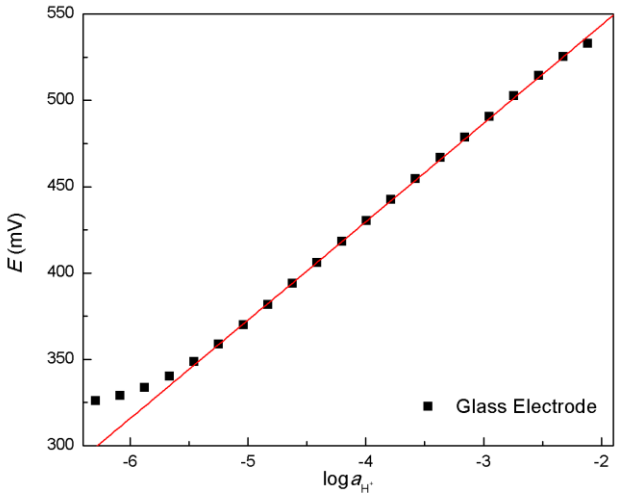

GCE/PEDOT:PSS (Calibration in KCl)

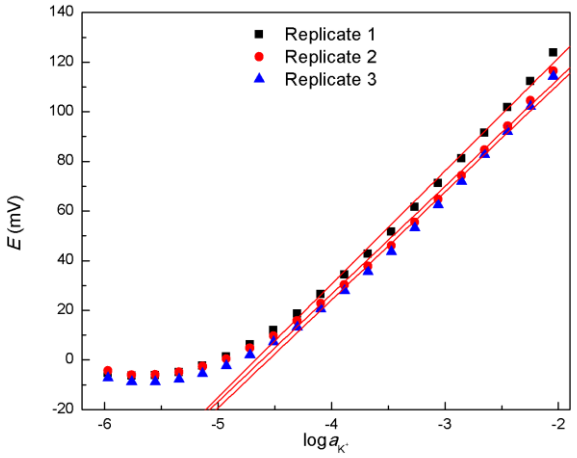

GCE/PEDOT:PSS (Calibration in HCl)

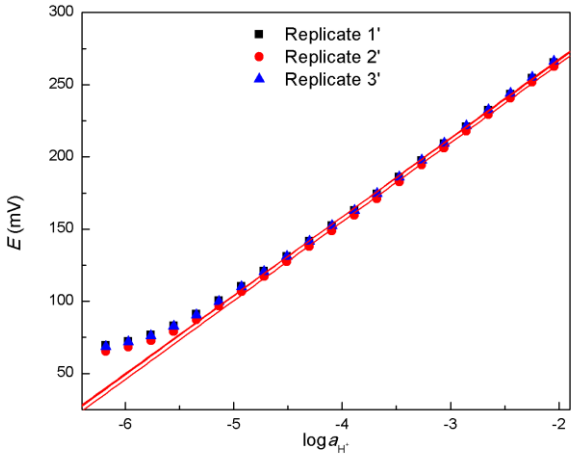

GCE/PEDOT:Cl$^-$ (Calibration in KCl)

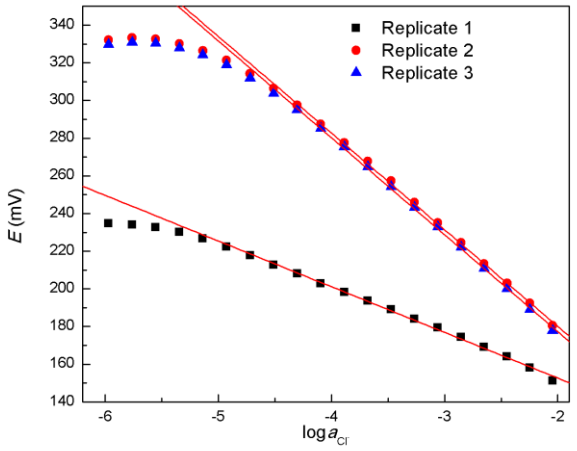

GCE/PEDOT:Cl$^-$ (Calibration in HCl)

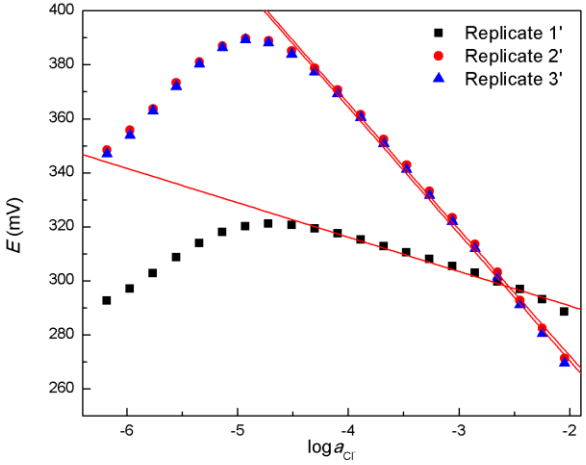

GCE/PEDOT:Cl^-/Cl^- ISM (without BE)

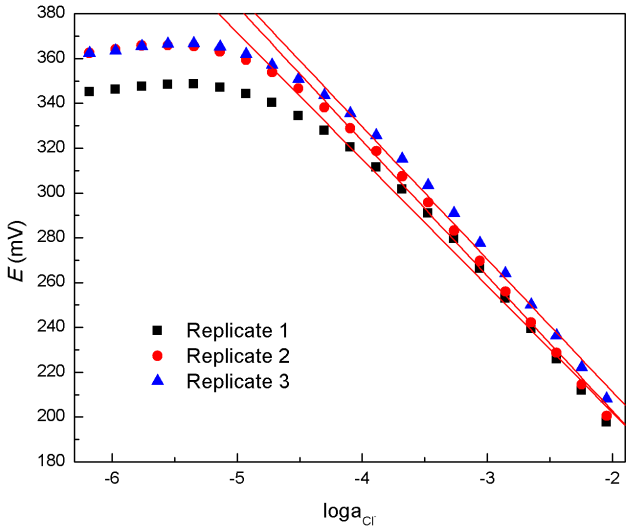

Appendix B.

Chronoamperograms and chronocoulograms of potassium, hydrogen and chloride SCISEs without background electrolyte (interfering ions). The measurements were performed at the open-circuit potential of each electrode, measured for 10 minutes prior to the chronoamperometric experiment. The current vs. time profile is represented by the black line, while the charge vs. time profile is depicted in blue. Every graph represents one electrode in the triplicate of electrodes prepared for the measurements (Replicate 2/2' on the left and Replicate 3/3' on the right). The changes in concentration, performed sequentially were of 5%, back and forth, from 1 mM to 1.05 mM and from 1.05 mM to 1 mM KCl (HCl), respectively

GCE/PEDOT:PSS/K^+ ISM

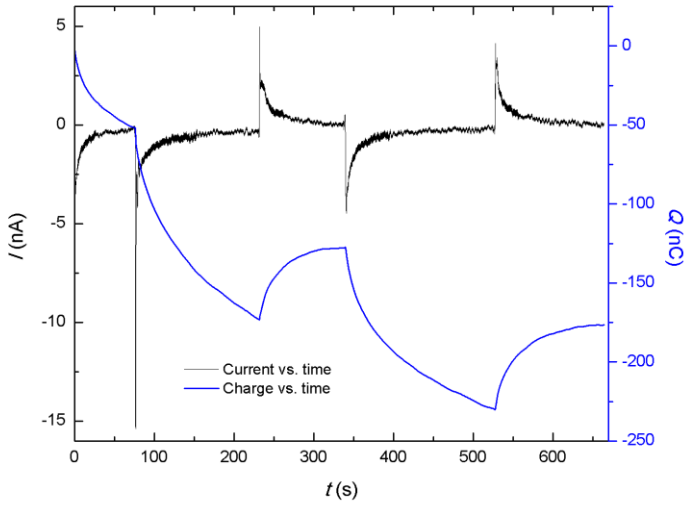

GCE/PEDOT:PSS/K^+ ISM

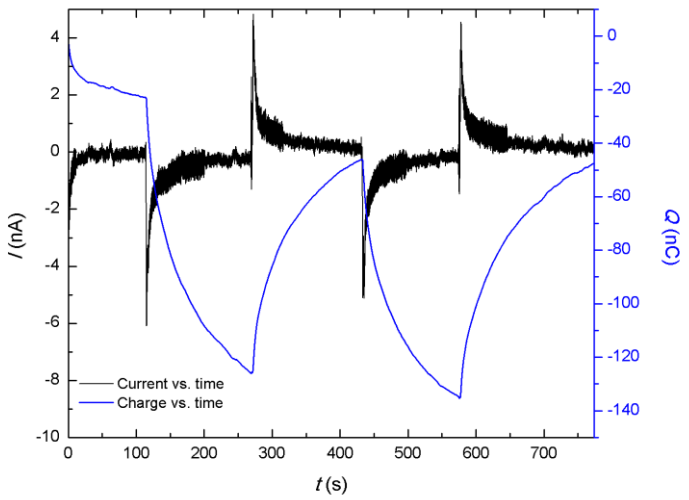

GCE/PEDOT:Cl^-/K^+ ISM

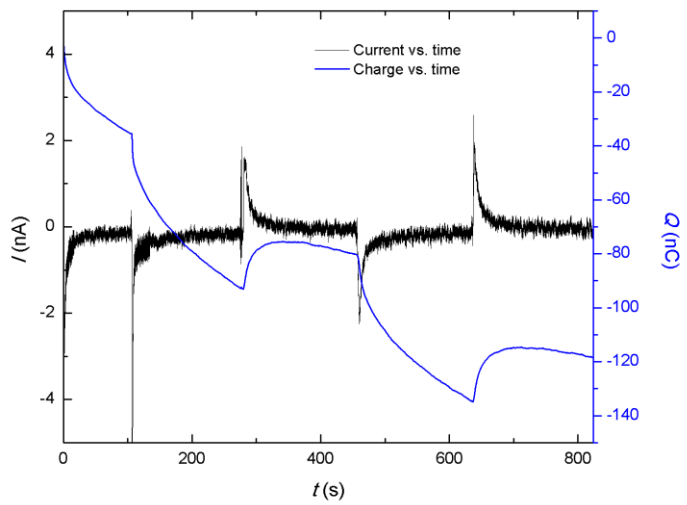

GCE/PEDOT:Cl^-/K^+ ISM

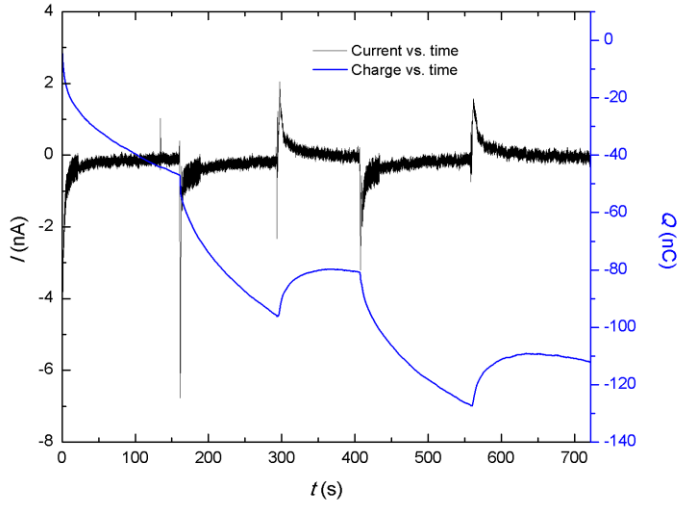

GCE/PEDOT:Cl^-/H^+ ISM

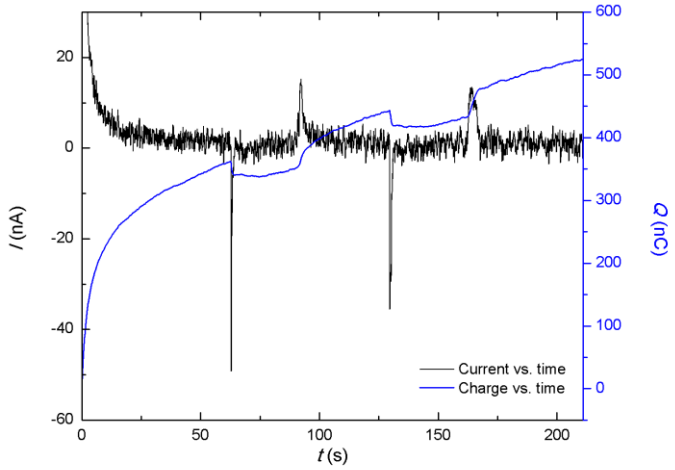

GCE/PEDOT:Cl^-/H^+ ISM

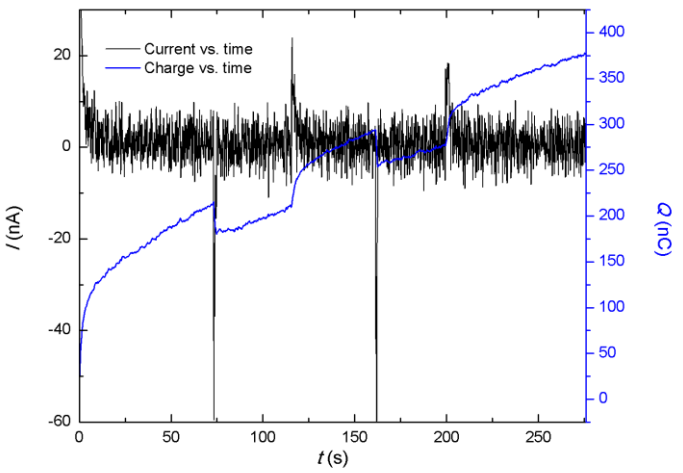

GCE/PEDOT:Cl⁻/Cl⁻ ISM

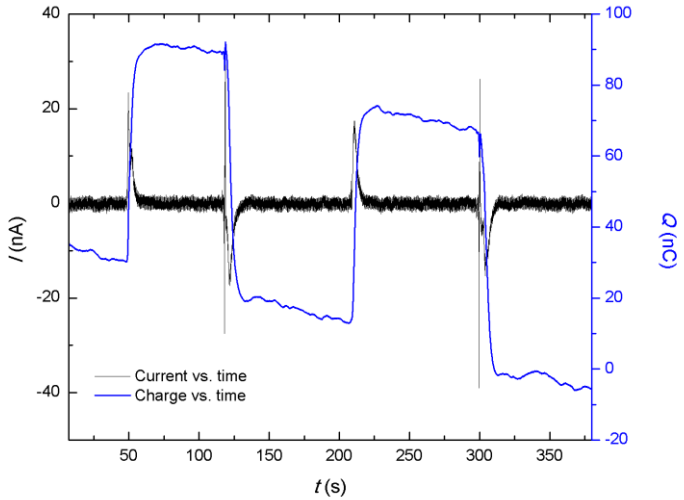

GCE/PEDOT:Cl⁻/Cl⁻ ISM

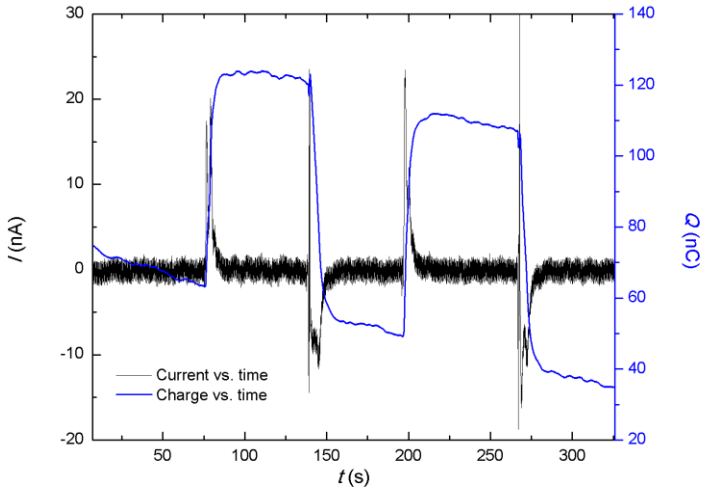

GCE/PEDOT:PSS in KCl

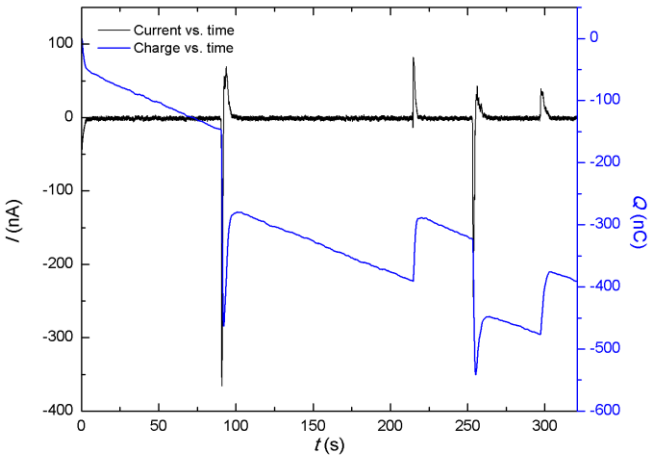

GCE/PEDOT:PSS in KCl

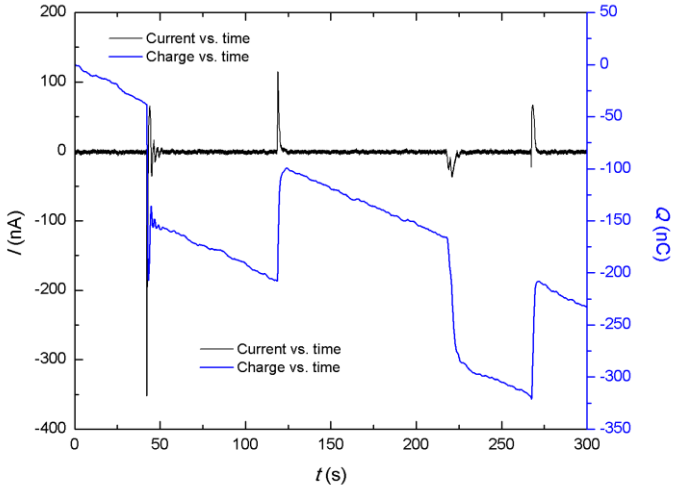

GCE/PEDOT:PSS in HCl

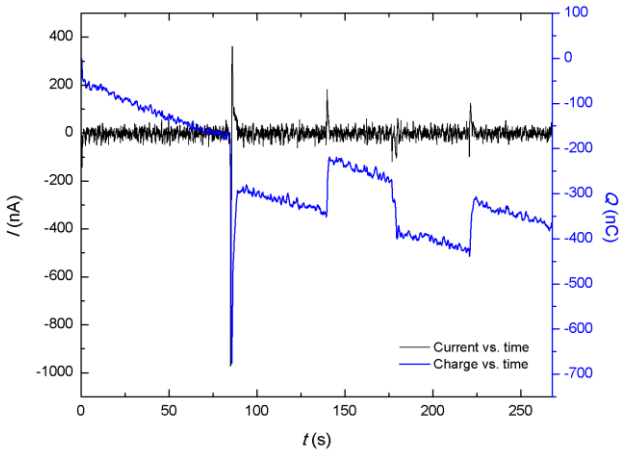

GCE/PEDOT:PSS in HCl

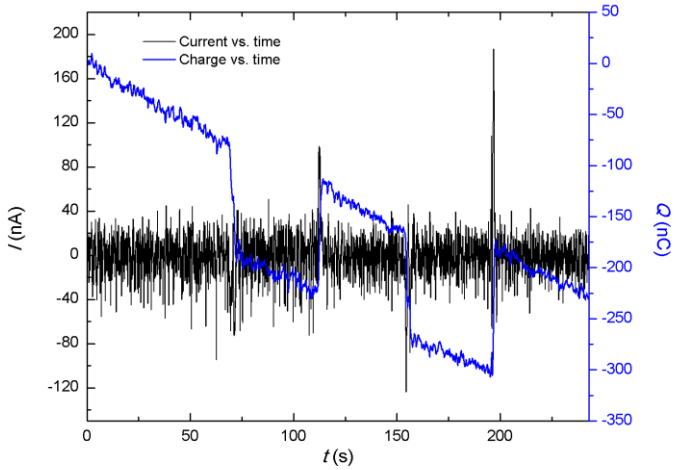

GCE/PEDOT:Cl$^-$ in KCl

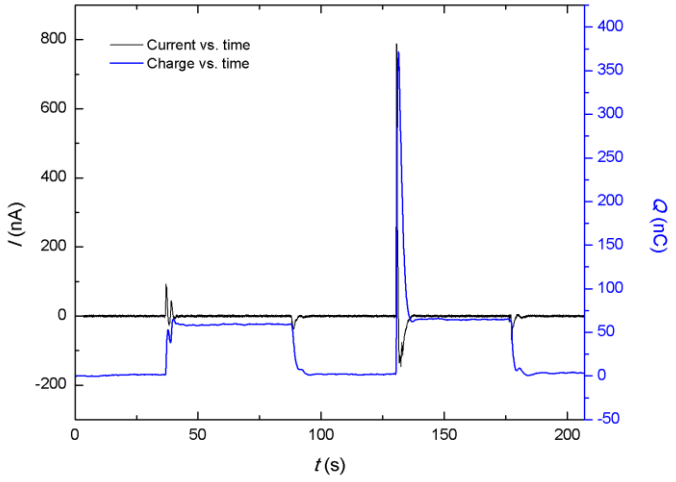

GCE/PEDOT:Cl$^-$ in KCl

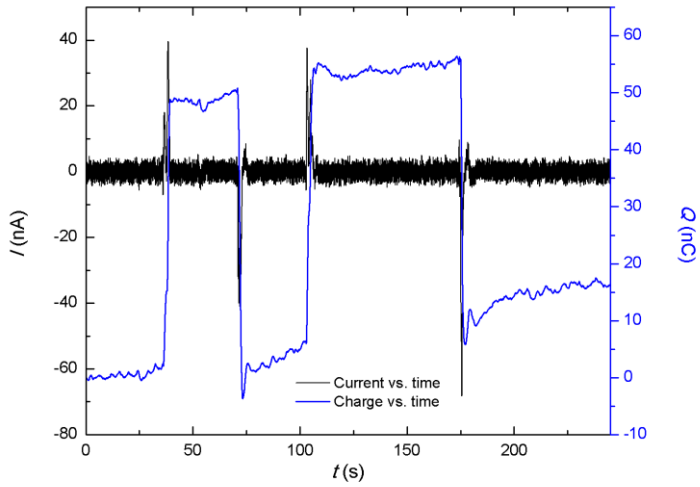

GCE/PEDOT:Cl⁻ in HCl

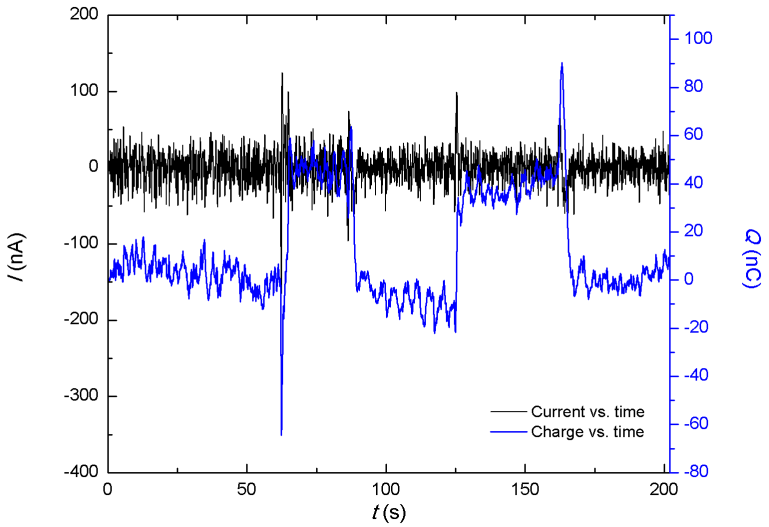

Appendix C.

Chronoamperograms and chronocoulograms of potassium SCISEs with background electrolyte (0.1 M NaCl). The measurements were performed at the open-circuit potential of each electrode, measured for 10 minutes prior to the chronoamperometric experiment. The current vs. time profile is represented by the black line, while the charge vs. time profile is depicted in blue. Every graph represents one electrode in the triplicate of electrodes prepared for the measurements (Replicate 2/2' on the left and Replicate 3/3' on the right). The changes in concentration, performed sequentially were of 5%, back and forth, from 1 mM to 1.05 mM and from 1.05 mM to 1 mM KCl (HCl), respectively

GCE/PEDOT:PSS/K^+ ISM

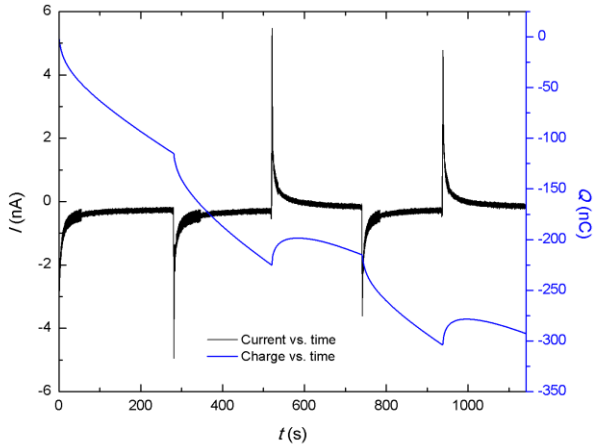

GCE/PEDOT:PSS/K^+ ISM

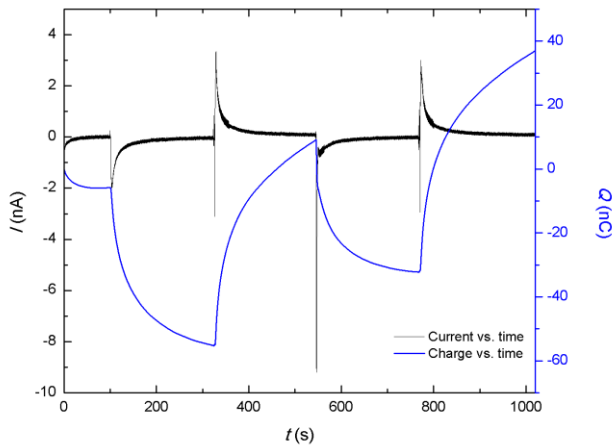

GCE/PEDOT:Cl^-/K^+ ISM

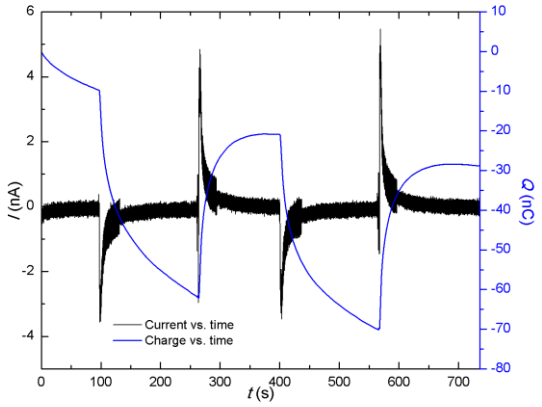

GCE/PEDOT:Cl^-/K^+ ISM

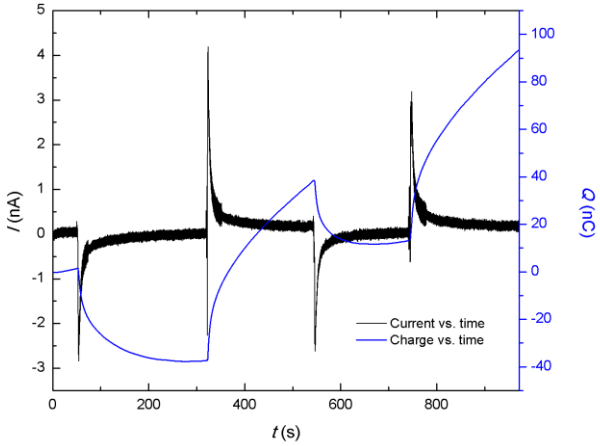

Appendix D

Water-layer test, performed by immersing the SCISEs in 0.1 M solution of the primary ion, followed by subsequent immersion into 0.1 M solution of the interfering ion and then back in 0.1 M solution of the primary ion

GCE/PEDOT:PSS/K^+ ISM

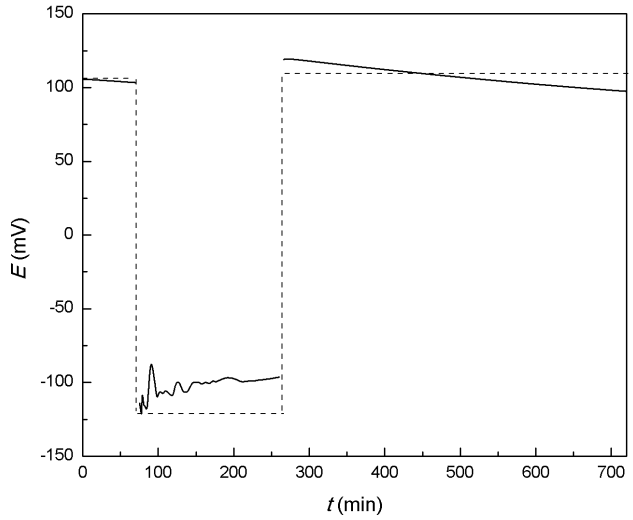

GCE/PEDOT:PSS/K^+ ISM

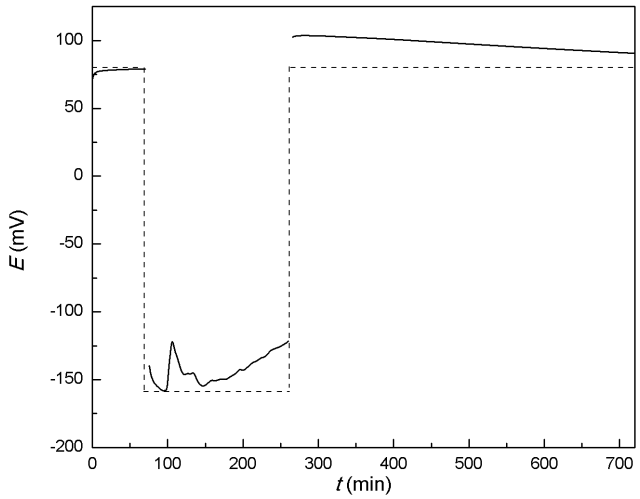

GCE/PEDOT:Cl^-/K^+ ISM

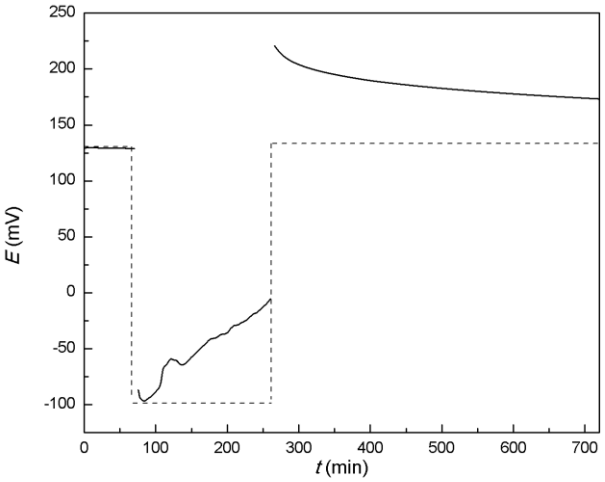

GCE/PEDOT:Cl^-/K^+ ISM

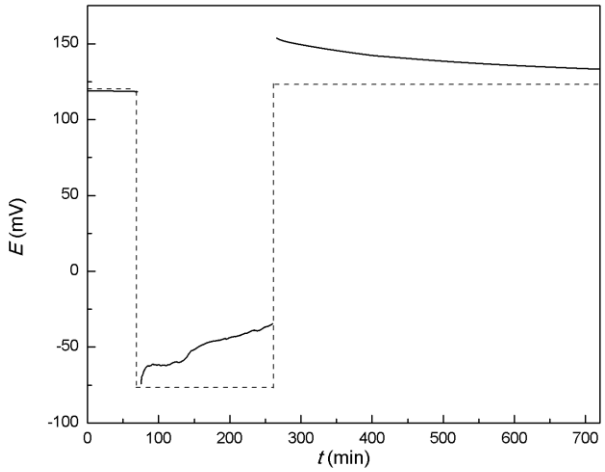

GCE/PEDOT:PSS/H^+ ISM

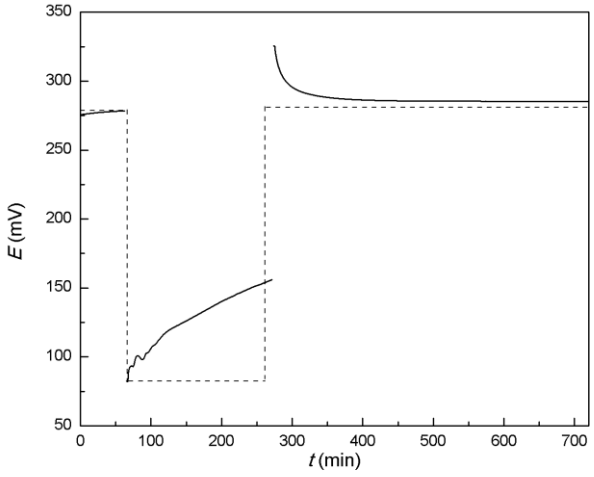

GCE/PEDOT:PSS/H^+ ISM

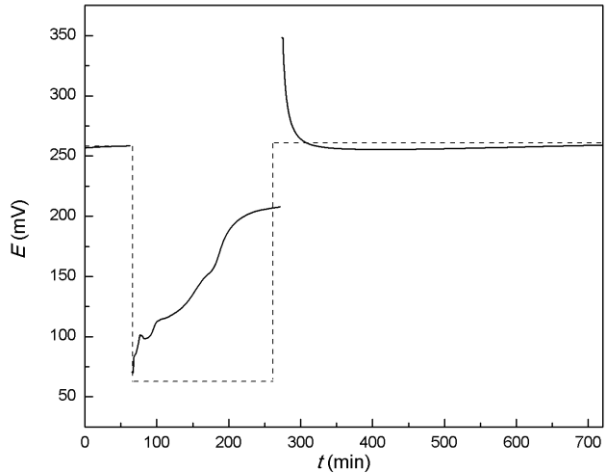

GCE/PEDOT:Cl^-/H^+ ISM

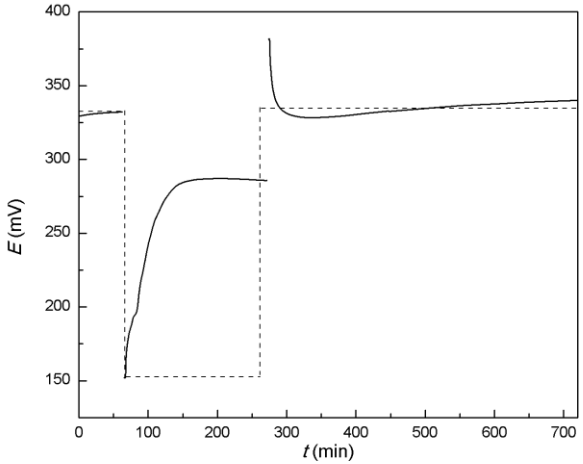

GCE/PEDOT:Cl^-/H^+ ISM

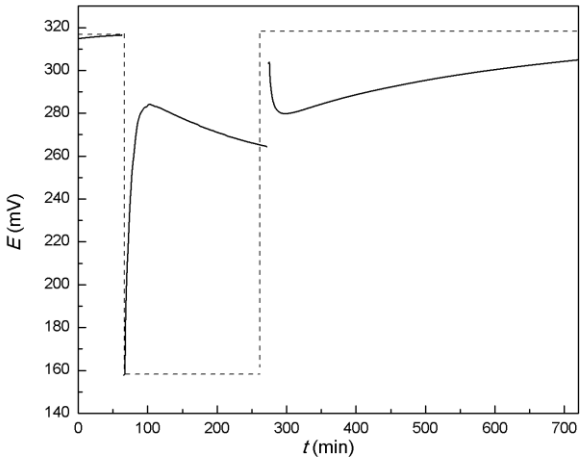

GCE/PEDOT:Cl^-/Cl^- ISM

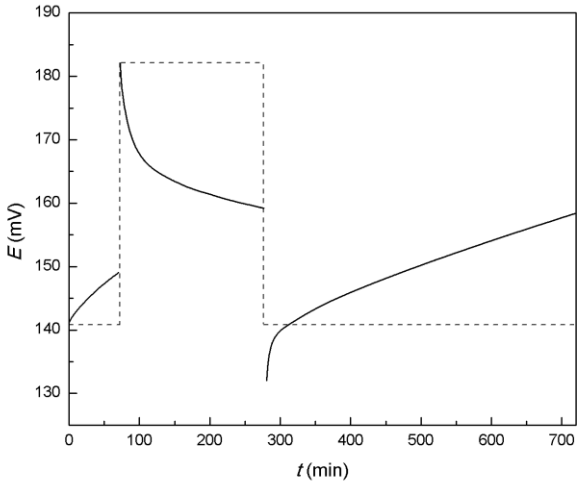

GCE/PEDOT:Cl^-/Cl^- ISM

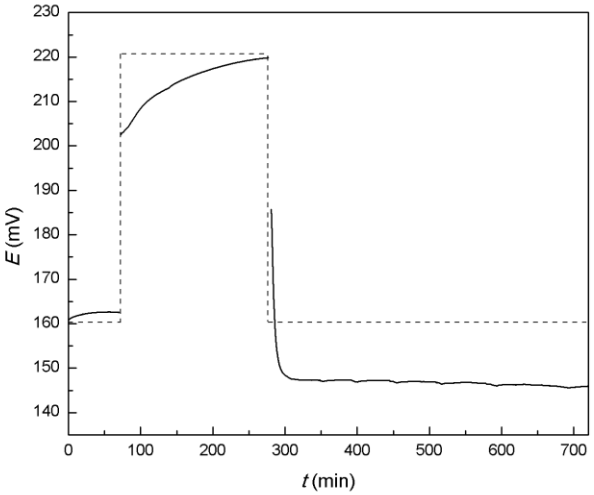

Appendix E

Resistance values (given in kΩ) of potassium, hydrogen and chloride SCISEs, determined from their respective electrochemical impedance spectra as the diameter of the high-frequency semicircle

Electrode	GCE/PEDOT:PSS/K^+ ISM	GCE/PEDOT:Cl^- /K^+ ISM	GCE/PEDOT:PSS/H^+ ISM	GCE/PEDOT:Cl^- /H^+ ISM	GCE/PEDOT:Cl^- /Cl^- ISM
Replicate 1	181	182	33	19	16
Replicate 2	213	205	29	22	19
Replicate 3	198	170	33	12	18
Average	197	186	32	18	18
s_d	16	18	2	5	2

Appendix F

Cyclic voltammograms of PEDOT:PSS and PEDOT:Cl- polymer films, recorded in 0.1 M KCl solution at 100 mV/s scan rate

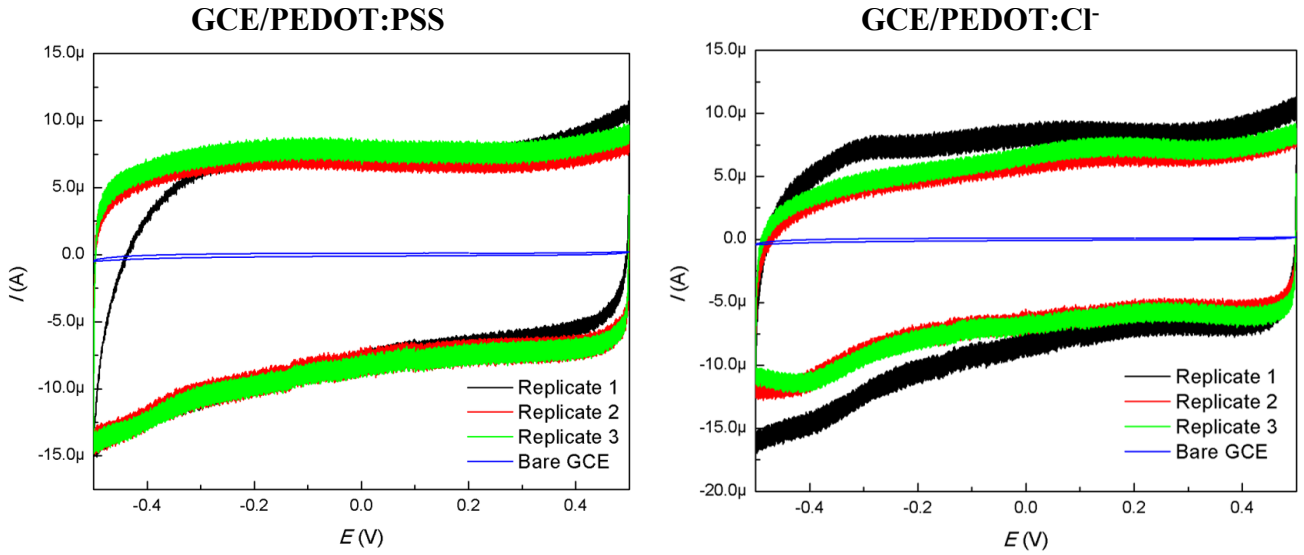

Appendix G

Equilibration times of potassium hydrogen and chloride SCISEs (given in seconds) in the presence, or without, the BE, determined at the 95% of the decay of the current peak in their respective chronoamperograms

Electrode	GCE/PEDOT:PSS/K^+ ISM		GCE/PEDOT:Cl^-/K^+ ISM		GCE/PEDOT:Cl^-/H^+ ISM	GCE/PEDOT:Cl^-/Cl^- ISM
	With BE	**No BE**	**With BE**	**No BE**	**No BE**	**No BE**
Replicate 1	60	61	69	70	10	7
	75	80	77	67	9	6
	84	74	79	65	11	5
Replicate 2	60	61	65	78	6	8
	62	65	66	62	7	6
	67	63	64	63	8	5
Replicate 3	65	72	62	61	5	7
	69	64	72	68	8	6
	81	78	82	67	9	8
	63	62	62	79	8	6
	60	59	64	63	8	6
Average	57	60	63	60	9	5
	67	67	69	67	8	6
s_d	9	9	7	7	2	1

Appendix H

Equilibration times (given in seconds) of PEDOT:PSS and PEDOT:Cl- modified GCEs, determined at the 95% of the decay of the current peak in their respective chronoamperograms

Electrode	GCE/PEDOT:PSS		GCE/PEDOT:Cl^-	
	In KCl	**In HCl***	**In KCl**	**In HCl***
Replicate 1	8	-	2	-
	6	-	1	-
	5	-	1	-
Replicate 2	6	-	1	-
	6	-	2	-
	8	-	1	-
	7	-	2	-
Replicate 3	6	-	2	-
	6	-	1	-
	5	-	2	-
	5	-	1	-
Average	7	-	2	-
	6	-	1	-
s_d	1	-	1	-

*The equilibration times were too fast to measure, less than a second